Ionics
https://doi.org/10.1007/s11581-025-06772-6

RESEARCH

Walrus optimization algorithm for enhanced solid oxide fuel cell (SOFC) model parameter identification

Manish Kumar Singla[1,2,3] · Manpreet Singh[1] · Ramesh Kumar[4,11] · Pradeep Jangir[5,6] · Arpita[7,10] · Reena Jangid[8,9]

Received: 17 July 2025 / Revised: 15 September 2025 / Accepted: 7 October 2025

Abstract

The growth of industrial and commercial fuel cell applications as a clean energy source is one of the focal points for energy sector researchers, leading to a constant search for cost-effective and accurate modeling techniques. This study meets this need by proposing a systematic method of determining solid oxide fuel cell (SOFC) stack models by appropriately choosing unknown parameters, where the main objective is to minimize the sum of squared errors between model output voltage and experimental data. The proposed walrus optimization (WO) algorithm is used to obtain an improved efficiency and better results. The reliability of the system is thoroughly tested in two cases, in which the temperature and pressure are varied (from 1073 to 1273 K and from 1 to 9 atm). A detailed comparative analysis with nine other metaheuristic algorithms proves the superior effectiveness of the proposed technique. The results show that the WO algorithm has significantly better performance and reaches the lowest mean squared error (MSE) values of 2.57E−07. Statistical analysis of 100 independent runs further confirms its outstanding stability as indicated by the smallest standard deviations (0.191 at 1073 K) and the shortest computational times, in the range of 0.20 to 0.41 s. The robustness of the algorithm is clearly proven by its top rank in the Friedman ranking test with a score between 1.125 and 1.5625 in all the test cases. These statistical results, along with the convergence and boxplot analyses, clearly demonstrate the excellent efficiency, precision, and reliability of the proposed WO-based technique for SOFC parameter identification.

Keywords Fuel cell · Optimization · Walrus optimization · Hydrogen cell · Run time · Convergence analysis

✉ Manish Kumar Singla
msingla0509@gmail.com

✉ Pradeep Jangir
pkjmtech@gmail.com

Manpreet Singh
drmanpreetsinghbfgi@gmail.com

Ramesh Kumar
rameshkumarmeena@gmail.com

Arpita
apyjangid@gmail.com

Reena Jangid
reenajangidiitm@gmail.com

[1] Baba Farid College of Engineering and Technology, Bathinda, Punjab 151001, India

[2] Department of Biosciences, Saveetha School of Engineering, Saveetha Institute of Medical and Technical Sciences, Chennai 602105, India

[3] Applied Science Research Centre, Applied Science Private University, Amman 11937, Jordan

[4] Chitkara University Institute of Engineering & Technology, Chitkara University, Rajpura, Punjab, India

[5] Department of Electronics and Communication Engineering, Chandigarh University, Mohali 140413, India

[6] Jadara University Research Center, Jadara University, Irbid 21110, Jordan

[7] Sharda School of Engineering and Sciences, Sharda University, Uttar Pradesh, Greater Noida 201310, India

[8] Department of CSE, Graphic Era Hill University, Dehradun, Uttarakhand 248002, India

[9] Department of CSE, Graphic Era Deemed to Be University, Dehradun, Uttarakhand 248002, India

[10] Department of Electrical and Electronics Engineering, J.J College of Engineering and Technology, Tiruchirappalli, India

[11] Department of Research, Manipal University Jaipur, Rajasthan, Jaipur, India

Published online: 27 October 2025

Nomenclature

Symbol/acronym	Description Unit
General constants and variables	
F	Faraday's constant C mol^{-1}
R	Universal gas constant J mol^{-1} K^{-1}
T	Absolute temperature K
t	Current iteration number
T_{max}	Maximum number of iterations
n	Number of experimental data points
n_{cell}	Number of cells in the SOFC stack
k	Index for data points
SOFC electrochemical model	
V_{cell}	Output voltage of a single SOFC V
V_{stack}	Output voltage of the entire stack V
E_0	Reversible standard potential V
E_{nernst}	Nernst potential V
P_{H_2}	Partial pressure of hydrogen atm
P_{O_2}	Partial pressure of oxygen atm
P_{H_2O}	Partial pressure of water vapor atm
$V_{activation}$	Activation overvoltage loss V
V_{ohmic}	Ohmic overvoltage loss V
$V_{concentration}$	Concentration overvoltage lossV
J_{load}	Load current density mA cm^{-2}
I_k	Load current at data point k A
A	Tafel slope (activation loss coefficient) V
$I_{0,\alpha}$	Anode exchange current density mA cm^{-2}
$I_{0,c}$	Cathode exchange current density mA cm^{-2}
R_{ohm}	Area-specific ohmic resistance kΩ cm^2
B	Empirical constant (concentration loss coefficient) V
I_L	Limiting current density mA cm^{-2}
J_{max}	Maximum current density mA cm^{-2}
$V_{sample,k}$	Experimentally measured voltage at point k V
$V_{opti,k}$	Model-predicted voltage at point k V
Optimization problem	
x	Decision vector of unknown parameters
$f(x)$	Objective function (MSE) V^2
MSE	Mean squared error V^2
SSE	Sum of squared errors V^2
Walrus optimization (WO) algorithm	
X	Population (matrix of candidate solutions)
X_i^t	Position of the i-th walrus at iteration t
X_{best}^t	Position of the best walrus at iteration t
X_{second}^t	Position of the second-best walrus at iteration t
F	Fitness values of the population
LB	Lower bound of the search space
UB	Upper bound of the search space
d	Number of dimensions (variables)
$Threat_{signal}$	Danger signal
$Security_{signal}$	Safety signal
$A,\ R$	Danger factors
α	Linearly decreasing control parameter
β	Migration step size control parameter
$Exploration_{step}$	Step size during migration (exploration)
$Male_i^t$	Position of the i-th male walrus
$Female_i^t$	Position of the i-th female walrus
$Juvenile_i^t$	Position of the i-th juvenile walrus
P	Distress coefficient for juvenile walruses
O	Reference safety position for juveniles
LF	Lévy flight random vector
$Levy(\alpha)$	Lévy flight distribution function
$\Gamma(z)$	Gamma function
α, b	Gathering coefficients
θ	Angle for gathering behavior
$r_1 r_2 r_3 r_4 r_5$	Uniformly distributed random numbers in (0, 1)
Performance metrics	
Min	Minimum MSE value found V^2
Max	Maximum MSE value found V^2
$Mean$	Average MSE value V^2
$Std.$	Standard deviation of MSE values V^2
RT	Average execution (run) time Seconds
FR	Friedman rank (lower is better)
Algorithm acronyms	
WO	Walrus optimization algorithm
ChOA	Chimp optimization algorithm
FOA	Following optimization algorithm
BOA	Butterfly optimization algorithm
AOS	Atomic orbital search
SCSO	Sand cat swarm optimization
SHO	Spotted hyena optimization
SOA	Seagull optimization algorithm
SSA	Salp swarm algorithm
WOA	Whale optimization algorithm
Other cited algorithms	
GWO	Grey wolf optimization
ACGWO	Adaptive chaotic grey wolf optimization
CSGWO	Cuckoo search-grey wolf optimization

MGWO	Modified grey wolf optimization
COA	Coyote optimization algorithm
BSSO	Binary shark smell optimization
CGFROA	Grass fibrous root optimization
MAVO	Modified African vulture optimization
ELM	Extreme learning machines
IRFO	Improved red fox optimizer
CHDJ	Competitive hybrid differential evolution and Jaya
CLDMMPA	Comprehensive learning dynamic multi-swarm marine predators algorithm
MPA	Marine predators algorithm
SCSO	Simplified competitive swarm optimizer
coRNA-GA	Co-evolution RNA genetic algorithm
ISO	Interior search optimizer
CGRA	Converged grass fibrous root optimization algorithm

Fuel cell types

SOFC	Solid oxide fuel cell
PAFC	Phosphoric acid fuel cell
MCFC	Molten carbonate fuel cell
PEMFC	Polymer exchange membrane fuel cell
DMFC	Direct methanol fuel cell
AFC	Alkaline fuel cell

General terms

NFL	No free lunch theorem
FRT	Friedman rank test
I-V curve	Current–voltage characteristic curve
P-V curve	Power–voltage characteristic curve

Introduction

The world's escalating electrical energy demand, driven by industrialization and civilization, currently relies heavily on fossil fuels [1]. However, concerns like global warming, resource depletion, and harmful emissions necessitate a shift towards sustainable and eco-friendly alternatives [2]. Renewable energy sources are increasingly popular, offering environmental benefits, minimal carbon emissions, and an inexhaustible supply. Within the renewable energy landscape, fuel cells have emerged as a compelling option over the last two decades, recognized for their high efficiency and emission-free operation in both small and large power generation [3–7]. Of the many types of phosphoric acid, molten carbonate, polymer exchange membrane, solid oxide, direct methanol, alkaline, and reversible fuel cells, the SOFC is a leading contender [8, 9]. SOFCs are highly favored for their high efficiency and operating temperature, along with their ability to directly use natural gas. Their advantages include robustness, CO insensitivity, high co-generation potential, fuel flexibility, and efficiencies of 60–70% even at high temperatures without needing catalysts [10]. These properties make SOFCs ideal for diverse applications such as transportation, waste-water treatment, distributed and co-generation, auxiliary power units, and space dmissions [11].

SOFCs are highly regarded by manufacturers as a promising solution for electricity generation due to their flexibility and rapid response. However, accurately predicting SOFC characteristics is difficult because they involve complex chemical and electrical processes. An accurate mathematical model is essential to evaluate SOFC performance under various conditions and optimize its design. A single SOFC's operation includes numerous intricate processes like electric charge transfer, heat transfer, electrochemical reactions, and mass transfer. These are collectively represented by a complex mathematical model [12, 13]. Among these, the electrochemical model is widely favored in research due to its effectiveness. Despite its utility, developing a precise electrochemical model for SOFCs remains a significant challenge for researchers globally, primarily due to its highly non-linear nature. The multi-variable, multi-modal complexity of SOFC mathematical models makes controlling and predicting their performance under varying conditions particularly hard. Moreover, these models contain several interdependent, unknown parameters that critically influence output performance, with even minor variations causing substantial effects. Manufacturers typically do not provide information on these parameters. Therefore, an optimal parameter identification approach is crucial for developing accurate SOFC models. Such models enable effective online control and facilitate performance assessment under diverse conditions like different loads, temperatures, and gas flow rates [14]. The behavior of SOFCs is characterized by polarization curves (current density vs. power and current density vs. voltage), which are derived from the mathematical model. These models comprise voltage equations representing open circuit voltage and various voltage drops (concentration, ohmic, and activation), all significantly impacted by the unknown parameters. Thus, parameter identification is vital to accurately model an SOFC and generate polarization characteristics that align with experimental data.

Many researchers have successfully identified and estimated SOFC parameters using metaheuristic algorithms. For instance, Guo et al. [15] utilized a modified fractional order dragonfly algorithm, minimizing the Sum of Squared Errors (SSE) between empirical and calculated data, and compared their results with other algorithms. Hao et al. [16] introduced an adaptive chaotic grey wolf optimization (ACGWO), an enhancement of the standard GWO, which demonstrated superior precision, robustness, and convergence speed

(based on MSE) for SOFC parameter identification. Bai et al. [17] proposed a hybrid cuckoo search-grey wolf optimization (CSGWO) for a 5-kW dynamic tubular stack. This approach, which used MSE as its objective function and was tested across varying pressures and temperatures, showed improved precision and convergence with lower MSE values compared to other algorithms. Similarly, Wang et al. [14] applied a modified grey wolf optimization (MGWO) to extract SOFC parameters, minimizing SSE. Their algorithm's reliability was confirmed under two different pressure and temperature scenarios, proving its accuracy against other well-known methods. Kele et al. [18] adopted a modified cat optimization algorithm to estimate 96-cell SOFC model parameters, minimizing the error between estimated and simulated output voltages. Their findings were benchmarked against algorithms like coyote optimization (COA), chaotic binary shark smell optimization (BSSO), grass fibrous root optimization (CGFROA), and modified African vulture optimization (MAVO). Zhang et al. [19] employed extreme learning machines (ELM) based on an improved red fox optimizer (IRFO) to estimate dynamic SOFC model parameters, using MSW as the objective function and comparing its effectiveness with existing literature. Xiong [20] introduced a novel competitive hybrid differential evolution and Jaya algorithm (CHDJ) for identifying parameters of tubular stacks and cylindrical cells at various temperatures and pressures. This algorithm, which used MSE, proved more effective with lower MSE values than other established algorithms. Finally, Yousri et al. [21] developed CLD-MMPA, a new variant of the marine predators algorithm (MPA) incorporating comprehensive learning and dynamic multi-swarm approaches to identify unknown parameters. Its performance was validated using steady-state and dynamic SOFC models, with non-parametric tests and statistical metrics confirming its effectiveness against other comparative algorithms. Ba et al. [22] optimized a Rotor Hopfield neural network using the Grey Wolf Optimization (GWO) algorithm to estimate model parameters. Their approach, based on an MSE objective function, yielded results that closely matched experimental data with reduced computational complexity. Xiong et al. [23] introduced a simplified competitive swarm optimizer (SCSO) to evaluate unknown parameters for both a 5-kW dynamic tubular stack and a Siemens cylindrical cell. Their findings showed that SCSO delivered superior accuracy, convergence, and robustness. Yang et al. [24] conducted a review analysis specifically on metaheuristic approaches for identifying SOFC parameters, summarizing the field's progress. Wei et al. [25] applied a chaotic binary shark smell optimizer to determine steady-state and dynamic model parameters, minimizing MSE as their objective function. Wang et al. [26] utilized a co-evolution RNA genetic algorithm (coRNA-GA) to identify unknown parameters for a 5-kW SOFC, comparing their results against other established algorithms. Hay et al. [27] employed an interior search optimizer (ISO) to estimate transient and steady-state SOFC model parameters, again using MSE as the objective. They also investigated oxygen and hydrogen flow rates, comparing their results with the grasshopper optimizer, satin bowerbird algorithm, and genetic algorithm. Yang et al. [28] adopted an extreme learning machine-based method for evaluating parameters of a 5-kW SOFC. Shi et al. [29] minimized the Sum of Squared Errors (SSE) between experimental and estimated SOFC model voltages at varying temperatures and pressures using a converged grass fibrous root optimization algorithm (CGRA). Abaza et al. [30] used a coyote optimizer to minimize the error in polarization characteristics, successfully evaluating unknown SOFC parameters.

While numerous metaheuristic algorithms, often in modified forms, have been used to accurately estimate unknown parameters in complex SOFC models, the non-linearity and complexity of these models still leave room to test the reliability of newer algorithms [31, 32]. Existing approaches continue to grapple with issues like poor convergence, sensitivity to control parameters, entrapment in local minima, high computational time, and inadequate exploration/exploitation balances [33–35]. Despite these challenges, the past two decades have seen the emergence of many new naturally inspired optimization algorithms, such as the Puma optimizer, Levy flight arithmetic algorithm, football training algorithm, and hiking optimization algorithm [36–41]. Additionally, several metaheuristic algorithms have been specifically enhanced for SOFC parameter estimation, including improved versions of cat and mouse optimization [42], repairable grey wolf optimizer [43], and co-operation search algorithm [44]. The precise and trustworthy determination of battery state of health (SOH) is a fundamental issue for the safety, durability, and performance of energy storage systems in applications from electric vehicles to grid storage. The complex non-linear degradation behavior of lithium-ion batteries is difficult to model using conventional techniques. As a result, highly effective solutions have emerged in the form of sophisticated data-driven techniques. Recent studies have shown the effectiveness of machine learning and optimization algorithms; for example, particle swarm optimization with extreme learning machines [45] and hybrid neural networks with feature fusion [46], to obtain high estimation accuracy. Furthermore, the recent development of deep transfer learning techniques shows great promise in allowing accurate prediction of SOH from minimal, short-term charging data [47], reflecting a general trend that is seeing intelligent algorithms revolutionize prognostics in green energy systems [48].

However, each of these algorithms solves non-linear and complex optimization problems based on its unique capabilities. This aligns with the "No Free Lunch" (NFL) theorem, which states that no single algorithm can offer the

universally best solution for every optimization problem [7]. Nevertheless, the recent development of many effective metaheuristic algorithms makes them promising tools for solving complex, non-linear optimization problems, like SOFC parameter identification.

The walrus optimization (WO) [49] algorithm is a novel metaheuristic inspired by the social behaviors of walruses, specifically their migration, breeding, roosting, and foraging. It models how danger and safety signals influence a walrus population's collective movement and decision-making, including the assumed roles and interactions among male, female, and juvenile walruses. The algorithm begins by randomly generating a population of potential solutions within a defined search space. Based on the calculated danger signal (which decreases linearly over iterations), the WO switches between exploration (walruses migrate to new solution areas when danger is high, with their positions updated by factors including two vigilante walruses) and exploitation (walruses "reproduce" when danger is low). The exploitation phase further incorporates a security signal that dictates whether individual walruses engage in roosting (male positions updated by Halton sequence for diversity, female positions influenced by male and best walrus, and juvenile positions adjusted to evade predation using a Lévy flight model) or foraging. Foraging itself involves two subprocesses: fleeing from threats (based on distance to the best walrus) and gathering (cooperative movement influenced by other walruses' locations and governed by specific weights and coefficients). Overall, the WO algorithm leverages these bio-inspired behaviors to effectively navigate the search space and find optimal solutions.

This work's main contribution is the proposed walrus optimization (WO) algorithm, which we thoroughly evaluated across ten diverse SOFC simulation scenarios covering a wide range of operating temperatures and pressures. Our comprehensive comparisons against nine other current algorithms demonstrated WO's superior performance and enhanced stability. Rigorous statistical validation using the Friedman rank test (FRT), mean squared error (MSE) analysis, runtime assessment, and boxplot variance analysis further confirmed WO's reliability and the consistency of its results. Moreover, the algorithm's design suggests its promising applicability to other complex energy systems and control engineering challenges.

The main contributions of this research are multi-faceted and are organized in order to provide comprehensive progress in the field of solid oxide fuel cell (SOFC) parameter identification.

First, this work presents a new application of the recently established walrus optimization (WO) algorithm to the complex and non-linear problem of SOFC parameter estimation. The WO algorithm is uniquely inspired by the social behaviors of walruses (including, but not limited to, migration, breeding, roosting, and foraging), and their responses to danger and safety signals. This bio-inspired approach offers a powerful mechanism for exploring the high-dimensional, multi-modal search space of SOFC models, effectively balancing global exploration and local exploitation to prevent premature convergence.

Second, the work outlines a rigorous and exhaustive evaluation framework, in which the proposed methodology is tested in ten different SOFC operational scenarios. This covers a large range of critical operating conditions, such as temperatures ranging from 1073 to 1273 K and pressures varying from 1 to 9 atm. Such a thorough analysis is to ensure that the results are not limited to one point of data but have broad applicability and are reliable under different conditions of real-world application.

Third, the performance of the WO algorithm is systematically benchmarked against nine other contemporary metaheuristic algorithms, including Chimp Optimization Algorithm (ChOA), Butterfly Optimization Algorithm (BOA), and Sand Cat Swarm Optimization (SCSO), among others. The superior efficacy of the WO is unequivocally proven using multiple quantitative measures. It always gives the smallest values of mean squared error (MSE) and represents the highest degree of accuracy in matching experimental voltage–current data. Furthermore, it has the best stability, which is proven by the lowest standard deviations over several runs and the shortest computational runtime, so it is extremely efficient.

Fourth, in addition to simple numerical comparison, the results are confirmed with extensive graphical and statistical analyses. The close agreement between the V-I and P-V curves produced by the WO-optimized model and the experimental data provides visual proof of the precision of the model in predicting these results. Convergence curves show the fast and stable convergence towards the optimal solution. Boxplot analyses of the distributions of MSE values over 100 independent runs are conclusive of the robustness and consistency of the algorithm with the narrowest interquartile ranges and no significant outliers. The statistical superiority of the WO is further formally confirmed by attaining the highest rank in the Friedman ranking test in all tested scenarios.

Finally, the structure of the paper is designed to give a clear and logical progression from the underlying motivation and literature review, to the mathematical formulation of the SOFC model, to the detailed explanation of the novel algorithm, and to the presentation of comprehensive results and discussion.

Mathematical modelling of SOFC

Modelling of SOFC

Fuel cells are essentially small, continuous electricity generators powered by a chemical reaction. Instead of combustion

like conventional engines, they operate similarly to batteries but require a constant input of fuel and oxygen. These clean and efficient devices produce electricity without releasing harmful greenhouse gases, making them environmentally friendly [50]. SOFCs are a kind of high-temperature fuel cell that operates at a very hot 1000 °C [51]. They utilize hydrogen as their fuel source and extract oxygen from the surrounding air. A typical SOFC consists of three primary components:

The anode chemical reaction is:

$$H_2 + O^2 \rightarrow H_2O + 2e^- \tag{1}$$

The cathode chemical reaction is:

$$\frac{1}{2}O_2 + 2e^- \rightarrow O^{2-} \tag{2}$$

The overall electrochemical reaction is:

$$H_2 + \frac{1}{2}O_2 \rightarrow H_2O \tag{3}$$

In a SOFC, the cathode is where oxygen molecules are reduced, turning into negatively charged oxygen ions. These ions have the unique ability to move through the electrolyte, while electrons are blocked. On the fuel side, known as the anode, hydrogen interacts with these oxygen ions, producing water vapor and freeing up electrons. These electrons then travel through an external circuit linking the anode and cathode, providing electricity to connected devices. A visual representation of a SOFC is provided in Fig. 1.

The output voltage (V_{cell}) of a single SOFC cell can be determined using Eq. (4) [52]. This calculation takes into account two main aspects: the Nernst potential E_{nernst}, representing the maximum theoretical voltage achievable based on the cell's chemical reactions, and the over-potential (V_{loss}), which accounts for voltage reductions caused by various inefficiencies within the fuel cell during energy conversion.

$$V_{cell} = E_{nernst} - (Alllossesinafuelcell) \tag{4}$$

The actual voltage a hydrogen/oxygen fuel cell produces under operating conditions is determined by the Nernst equation (Eq. (5)). This equation accounts for factors influencing the cell's performance, such as temperature, pressure, and the concentrations (or partial pressures) of the reactants and products.

$$E_{nernst} = E_o + \frac{RT}{2F} ln\left(\frac{P_{H2} \times \sqrt{P_{O2}}}{P_{H2O}}\right) \tag{5}$$

The reversible standard potential (E_o) represents the theoretical maximum voltage a cell can produce under ideal conditions. The universal gas constant (R) relates temperature, pressure, and the amount of gas, while the Faraday constant (F) connects electrical charge to the extent of chemical reaction. These constants are crucial for understanding and calculating the performance of electrochemical cells, including fuel cells, by considering factors like temperature, pressure, and reactant concentrations in equations such as the Nernst equation. SOFCs suffer from three primary voltage losses that hinder their efficiency:

Activation loss: This initial energy barrier must be overcome before the fuel and oxygen can react. Operating conditions significantly impact this loss, which can be calculated using the Butler–Volmer equation (Eq. (6)).

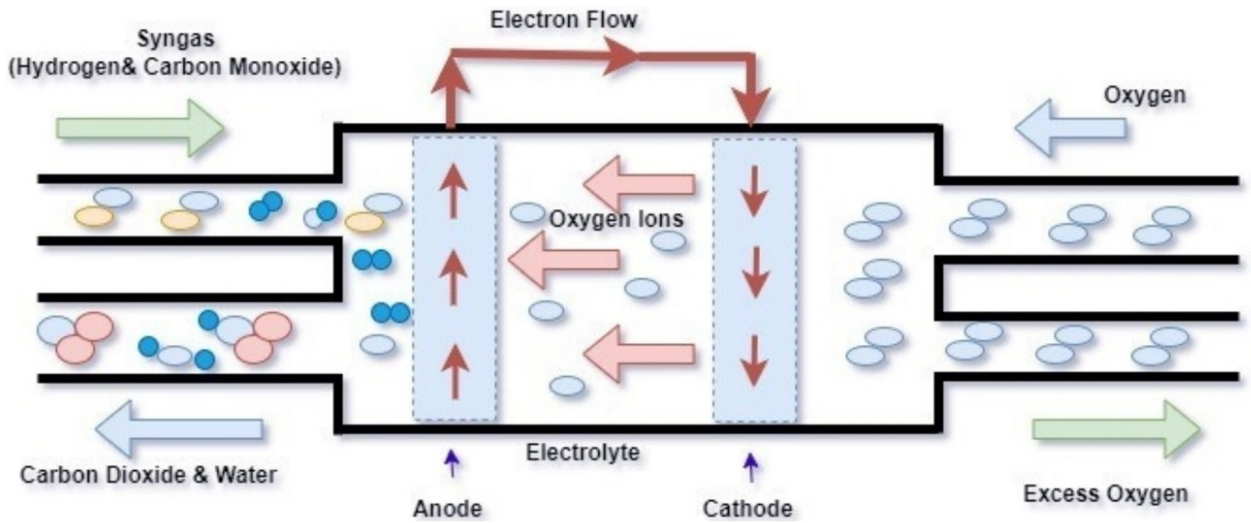

Fig. 1 SOFC diagram

Ohmic loss: Analogous to electrical resistance, the SOFC's materials resist the flow of ions, causing a voltage drop. This loss is dependent on the operating temperature and specific materials used in the cell.
Concentration over-potential loss: When the demand for fuel or oxygen at the electrodes exceeds the supply, concentration over-potential loss occurs. This can be triggered by high current draw or limitations in gas flow.

$$V_{activation} = Asinh^{-1}\left(\frac{J_{load}}{2J_{o,a}}\right) + Asinh^{-1}\left(\frac{J_{load}}{2J_{o,c}}\right) \quad (6)$$

where J_{load}, $J_{\text{o,a}}$ and $J_{\text{o,c}}$ are the load current density, anode exchange current density, and cathode exchange current density, in mA/cm^2, respectively. The slope of the Tafel line is represented by the symbol A.

The flow of ions through the electrolyte and electrons through the electrodes in an SOFC is hindered by inherent resistance. This resistance causes a voltage drop, known as ohmic loss, which can be calculated using Eq. (7).

$$V_{ohmic} = J_{load}R_{ohm} \quad (7)$$

where the ionic resistance is denoted by R_{ohm}.

The uneven distribution of reactants and products within the SOFC, known as concentration gradients, hinders the electrochemical reactions. This leads to a voltage drop, termed concentration loss (Vconcentration). As the operational current density approaches its maximum limit (Jmax), the effect of concentration loss becomes increasingly significant, as described by Eq. (8).

$$V_{concentration} = -b \times ln\left(\left(J_{max} - J_{load}\right)/J_{max}\right) \quad (8)$$

where b is an unknown parametric coefficient that varies depending on the operating parameters of the fuel cell.

The activation overpotential, represented by Eq. (6), is derived from the Butler–Volmer equation, which describes the kinetics of electrochemical reactions at the electrodes. This formulation is a standard approach for modeling the voltage loss due to the energy barrier of the charge transfer reaction and is well-established in the literature [28]. The ohmic loss, given by Eq. (7), is calculated from Ohm's law, where the voltage drop is directly proportional to the current density and the area-specific ionic resistance of the cell components [30]. The concentration overpotential, expressed in Eq. (8), is modeled based on the logarithmic expression for mass transport limitations, which becomes significant as the current density approaches the limiting current density [42]. The empirical constant b in Eq. (8) is a parametric coefficient that quantifies the magnitude of the concentration loss. Its value is not fixed and is highly dependent on several operating parameters of the fuel cell. Primarily, operating temperature exerts a significant influence; higher temperatures generally enhance gas diffusivity, potentially reducing the value of b. Conversely, operating pressure affects gas concentrations and diffusion rates, thereby influencing the concentration polarization and the value of b. Furthermore, the composition and flow rates of the fuel and oxidant gases directly impact reactant availability at the triple-phase boundaries. A lower fuel concentration or a lower flow rate can exacerbate concentration gradients, leading to a higher value of b. The microstructural properties of the electrodes, such as porosity and tortuosity, which are often considered fixed for a given cell but can vary between designs, also determine the resistance to mass transport and consequently affect the value of b. Therefore, the accurate identification of this parameter for a specific SOFC under its unique operating conditions is critical for developing a precise mathematical model.

The overall voltage output of an SOFC stack composed of n series-connected cells is determined by Eqs. (9–10). The dominant voltage losses in a fuel cell are activation, ohmic, and concentration losses. Secondary losses, though present, are relatively small and have a minimal effect on the overall performance of the SOFC.

$$V_{cell} = E_{nernst} - \left(V_{activation} + V_{ohmic} + V_{concentration}\right) \quad (9)$$

$$V_{stack} = n_{cell} \times V_{cell} \quad (10)$$

Formulating the issue

Prior to employing optimization algorithms for SOFC model parameter identification, two fundamental aspects need to be addressed. The first is the crucial step of defining the specific parameters that will be estimated. In the updated electrochemical model shown in Eq. (10), there are seven parameters that are considered unknown and therefore need to be determined through calibration. These parameters include the open-circuit voltage (E_0), the Tafel slope (A), the exchange current densities at the anode ($I_{0,a}$) and cathode ($I_{0,c}$), the area-specific resistance (R_{ohm}), the empirical constant (B), and the limiting current density (I_L). These seven parameters together form the decision vector:

$$x = \left[E_0, A, I_{0,c}, R_{\text{ohm}}, B, I_L, I_{0,a}\right] \quad (11)$$

The next crucial step is defining an appropriate objective function to guide the optimization. When identifying parameters for SOFC models, the main goal is to minimize the difference between the output voltages observed in experiments and those calculated by the model. To accomplish this, the mean squared error (MSE) is selected as the objective function, as explained in detail in [53]:

$$f(x) = \frac{1}{n}\sum_{k=1}^{n}\left(\text{error}_k\right)^2 = \frac{1}{n}\sum_{k=1}^{n}\left(V_{\text{sample},k} - V_{\text{opti},k}\right)^2 = \frac{1}{n}\sum_{k=1}^{n}\left[V_{\text{sample},k} - N_{\text{cell}}\left(E_0 - A\text{sinh}^{-1}\left(\frac{I_k}{2I_{0,a}}\right) - A\text{sinh}^{-1}\left(\frac{I_k}{2I_{0,c}}\right) - I_k R_{\text{ohm}} + B\ln\left(1 - \frac{I_k}{I_L}\right)\right)\right]^2 \tag{12}$$

The minimization of this objective function is performed under the constraint that the current density (I_k) at each data point considered must remain below the specified limiting current density (I_L):

$$I_k < I_L, k = 1, \ldots, n \tag{13}$$

Within this formulation of the mean squared error (MSE), n represents the total count of experimental data points used for parameter identification, $V_{\text{sample},k}$ denotes the experimentally measured voltage for the k-th data point, and $V_{\text{opti},k}$ is the corresponding voltage predicted by the SOFC model at the same current density I_k. The term N_{cell} indicates the total number of individual cells in the SOFC stack. Furthermore, to ensure that the model adheres to physically realistic electrochemical behavior, the constraint $I_{0,a} > I_{0,c}$ is additionally enforced, as suggested in reference [54].

The main aim of the optimization is to reduce the objective function $f(x)$, which quantifies the overall difference between the voltages predicted by the model and the real (experimental) voltage values. Ideally, if the model perfectly matched the experimental data, the objective function would be zero. However, in reality, due to inherent measurement errors and numerical estimations, achieving a very small, non-zero value for the objective function is usually considered a better result.

Algorithm (walrus optimization (WO))

Key biological principles

Apart from whales, the walrus is the ocean's largest mammal. Primarily inhabiting temperate to Arctic waters, walruses are social, amphibious creatures. Their herds can range from a few dozen to thousands. Characterized by a stout, cylindrical, and somewhat obese body with a flat head and blunt snout, they possess around 400 sensitive whiskers on their upper lip. Their most distinctive feature is a pair of continuously growing white upper canine teeth, forming tusks used for defense, foraging for clams, shrimp, and crabs in mud and sand, and aiding in ice climbing [55]. Despite their bulky appearance and massive bodies, walruses exhibit surprising flexibility in the water. Within the vast array of marine life, they stand out as exceptional divers, capable of submerging for up to 20 min and reaching depths of 500 m. Remarkably, they can remain on the seabed for as long as 2 h before needing to surface, a process they can accomplish in under three min.

The Walrus Optimization (WO) Algorithm is inspired by some of the social and survival behaviors of walrus populations that are directly analogous to the process of optimizing complex, non-linear systems such as solid oxide fuel cells (SOFCs). Specifically, the algorithm simulates four important behaviors of walruses—migration, breeding, roosting, and foraging—each of which represents a different phase in the optimization process. Migration is done under high perceived danger, causing the population to explore new areas of the solution space, similar to walruses moving to safer habitats. This exploration phase ensures a wide coverage of the parameter search space, which is critical for avoiding local optima in the highly multimodal SOFC parameter identification problem. On the other hand, under safer conditions, walruses will undertake breeding activities, which in the algorithm correspond to exploitation strategies: roosting and foraging. Roosting includes position updates according to social hierarchies (male, female, and juvenile dynamics), improving local search capability and population diversity (mechanisms like Halton sequences and influence from leading individuals). Foraging, which is sub-divided into fleeing from threats and gathering around resources, provides for refined local search and convergence towards optimal solutions. These biologically inspired mechanisms work together to achieve an effective balance between exploration and exploitation, similar to the adaptive response of the walrus to environmental cues. This balance is important for the accurate identification of seven interdependent parameters of the SOFC model because it guarantees robust convergence to globally optimal solutions while ensuring stability under varying operation conditions such as temperature and pressure.

Walruses exhibit a strong sense of community, and this is illustrated by:

- As the breeding season commences, walruses establish territories along the beach [56]. Dominant males secure the most advantageous locations, and the size of a male's territory is proportional to the number of females within his group.
- Adapted to the perpetually dark depths of the ocean where sunlight doesn't penetrate, walruses, similar to bats and dolphins, have limited specialized vision. Instead, they depend on echolocation for hunting and

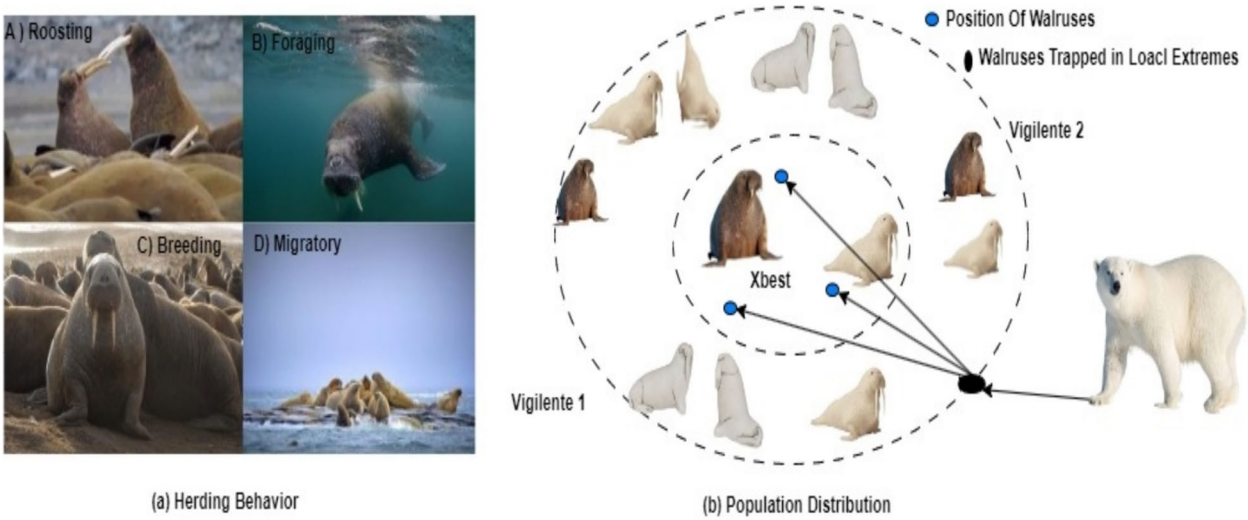

Fig. 2 Walrus herding behavior and population distribution

communicate with each other to share information about food sources.

- Demonstrating strong social bonds, walruses collectively defend against killer whales and readily come to the aid of their injured. Their history of enduring survival challenges has instilled a constant state of alertness [57], leading to behaviors like two walruses acting as guards prepared to assist any wounded individuals.

Drawing inspiration from the migratory, breeding, roosting, and foraging behaviors of walruses (as depicted in Fig. 2), the author introduces a novel metaheuristic algorithm, WO, for the first time. The author must clarify two key assumptions at this point:

- Danger and safety signals influence how walrus populations perceive and respond to the collective behavior of their members.
- The walrus algorithm models the behavioral and role divisions observed in walrus populations. Specifically, it incorporates the assumed social structures and interactions among male, female, and juvenile walruses.

In the mathematical framework of WO, the search space defines the boundaries within which the algorithm seeks the optimal solution. This is typically a multidimensional space composed of the problem's decision variables. The solution space encompasses all possible solutions, where each solution is represented by a walrus's position within the search space. This position, often a vector with components corresponding to the values of the decision variables (determined by the problem itself), signifies a potential solution. Ultimately, WO aims to identify the best solution within this search space—the one that optimizes the problem's objective function.

A computational approach based on a mathematical model

The starting phase

At the outset of the WO process, a collection of potential solutions (X) is randomly generated to serve as the starting point for the optimization, as shown in Eq. (14).

$$X = LB + rand(UB - LB) \tag{14}$$

In this context, LB and UB denote the lower and upper bounds for the problem variables, while 'rand' signifies a vector containing random values drawn from a uniform distribution between 0 and 1.

In the WO algorithm, each walrus represents an agent actively involved in the optimization process. Throughout the algorithm's iterations, the positions of these agents are continuously adjusted as shown in Eq. (15).

$$X = \begin{bmatrix} X_{1,1}X_{1,2} \ldots X_{1,d} \\ X_{2,1}X_{2,2}..X_{2,d} \\ \ldots \\ \ldots \\ X_{n,1}X_{n,2}..X_{n,d} \end{bmatrix}_{n \times d} \tag{15}$$

In this context, 'n' refers to the number of individuals in the population, and 'd' indicates the number of dimensions or design variables in the problem.

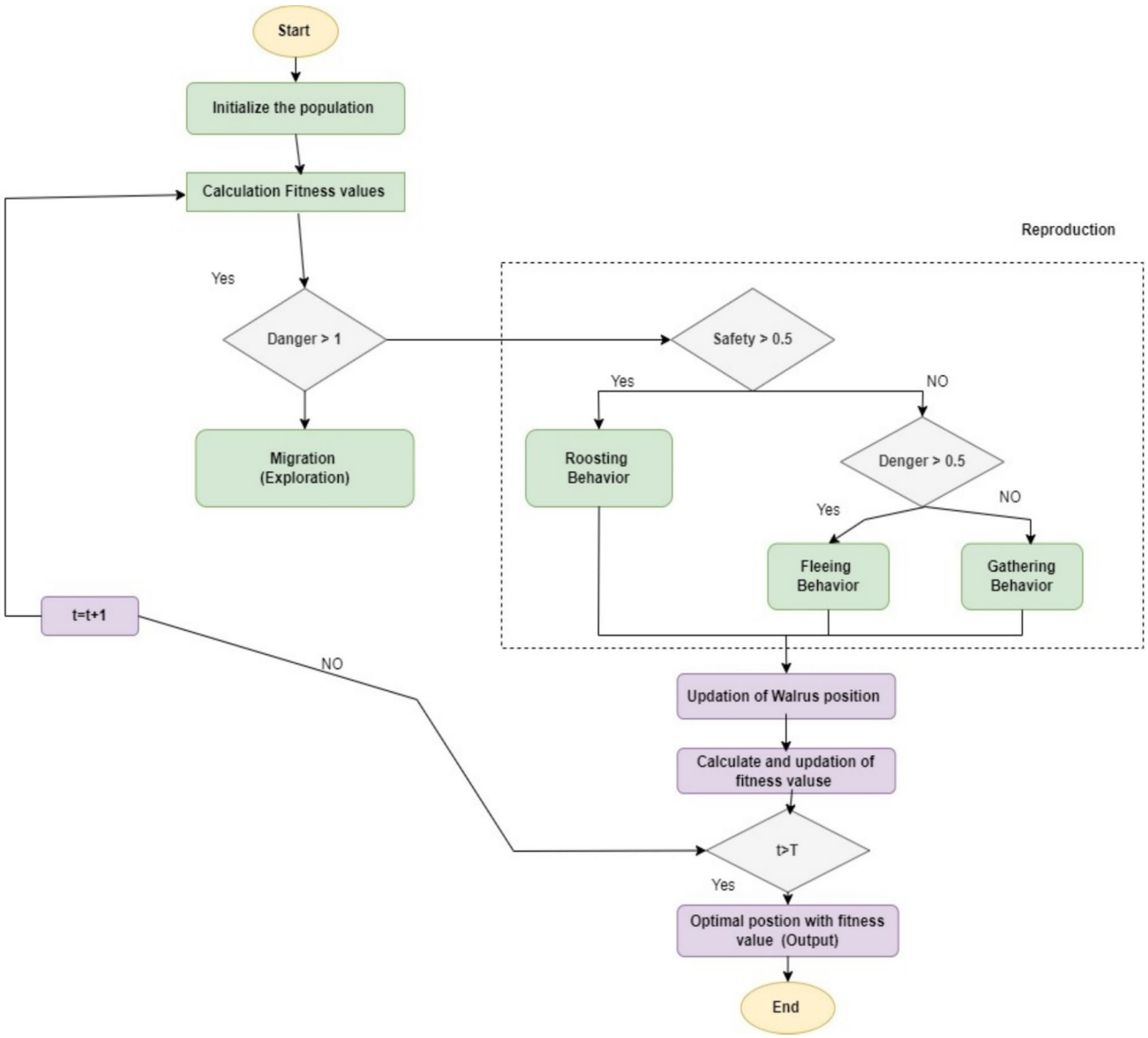

Fig. 3 Flowchart of Proposed Algorithm

The following structure is used to store the fitness values associated with every search agent, as shown in Eq. (16):

$$F = \begin{bmatrix} f_{1,1} f_{1,2} \cdots f_{1,d} \\ f_{2,1} f_{2,2} \cdot f_{2,d} \\ \cdots \\ \cdots \\ f_{n,1} f_{n,2} \cdot f_{n,d} \end{bmatrix}_{n \times d} \tag{16}$$

Adult walruses constitute 90% of the population, while juveniles make up the remaining 10%. Among these adults, the sex ratio is balanced, with one male for every female (1:1).

Indications of threat and security

Exhibiting significant vigilance during foraging and roosting, walrus populations employ one or two individuals as guards to patrol the area. Upon detecting any unusual activity, these guards promptly emit danger signals. Within the WO algorithm, the concepts of danger and safety signals are mathematically defined as Eq. (17-20):

$$Threat_{signal} = A * R \tag{17}$$

$$\alpha = 1 - t/T \tag{18}$$

$$A = 2 \times \alpha \tag{19}$$

$$R = 2 \times r_1 - 1 \tag{20}$$

where A and R represent danger factors. The parameter α linearly decreases from an initial value of 1 to 0 as the current iteration 't' progresses towards the maximum number of iterations 'T'.

In the WO algorithm, the safety signal, which complements the danger signal, is defined as shown in Eq. (21):

$$Security\_signal = r_2 \tag{21}$$

In this context, r_1 and r_2 represent random numbers that are uniformly distributed within the open interval (0, 1).

Exploration and diversification

When the perceived danger level becomes excessively high, walrus herds will migrate to regions offering better conditions for the population's survival. During this migration phase, a walrus's position is updated according to the following formula as shown in Eqs. (22–24):

$$X_{i,j}^{t+1} = X_{i,j}^{t} + Exploration\_step \tag{22}$$

$$Exploration\_step = \left(X_m^t - X_n^t\right) \bullet \beta \bullet r_3^2 \tag{23}$$

$$\beta = 1 - \frac{1}{1 + exp\left(-\frac{t-\frac{T}{L}}{T} \times 10\right)} \tag{24}$$

In this equation, $X_{i,j}^{t+1}$ denotes the new coordinate of the i-th walrus along the j-th dimension at the next iteration. $X_{i,j}^{t}$ is its current coordinate in the same dimension. The 'Migration step' refers to the distance the walrus moves. Two randomly selected vigilantes from the population have positions X_m^t and X_n^t. The parameter β controls the size of the migration step and varies smoothly as the iteration progresses. Finally, r_3 is a random value drawn from a uniform distribution between 0 and 1.

Table 1 SOFC operating conditions

Parameter	Cell number	Inlet air temperature (K)	Anode pressure (atm)	Cathode pressure (atm)	Inlet fuel temperature (K)
Values	96	1173	3	3	1173
Parameter	Air mass flow rate (mol/s)	Load current (A)	H_2 mass flow rate (mol/s)	H_2O mass flow rate (mol/s)	
Values	12.0×10^{-3}	0–158	0.9×10^{-3}	1.0×10^{-4}	

Table 2 Upper and lower bounds

Parameter	$I_L mA \bullet cm^{-2}$	$R_{ohm} k\Omega \bullet cm^2$	$A(V)$	$I_{0,a} mA \bullet cm^{-2}$	$I_{0,c} mA \bullet cm^{-2}$	$E_0(V)$	$B(V)$
Range	[0, 200]	[0, 1]	[0, 1]	[0, 30]	[0, 30]	[0, 1.2]	[0, 1]

Table 3 Model parameters and performance metrics

Algorithm	ChOA	FOA	BOA	AOS	SCSO	SHO	SOA	SSA	WOA	WO
E_0(V)	0.9708	1.109831	0.929422	1.112442	1.116785	1.045883	1.115058	1.104507	1.111326	1.114473
A(V)	0	0.179178	0	0.157573	0.017888	0.030521	0	0.017056	0.172366	0.036226
$I_{0,c}$(mA.cm^{-2})	12.23194	30	0.929422	24.74029	4.4028	30	1.232751	3.716976	29.2844	6.772891
R_{ohm}(kΩ·cm^2)	0	0	0	1.87E−05	0.004534	0	0.006561	0.004858	7.59E−05	0.004003
B(V)	0.570646	0.15475	0.456625	0.191022	0.056017	0.673995	0	0.047481	0.167224	0.065285
I_L(mA.cm^{-2})	198.8572	165.2318	183.0804	169.6338	159.3915	200	185.9326	159.0377	167.3338	159.8733
$I_{0,a}$(mA.cm^{-2})	28.8022	30	4.516596	29.33161	6.370626	30	22.09574	59.18456	29.90761	27.41861
Min	30.85847	0.223249	41.46445	0.217359	0.012631	31.35651	10.54381	0.152607	0.176223	**2.57E−07**
Max	**4235.352**	18.10158	226.9938	1.527961	0.676949	4236.134	226.9938	15.7283	1.755826	27.76684
Mean	1588.478	4.181744	155.3382	1.059947	0.434434	1686.361	130.1042	2.906668	0.518107	**0.704236**
Std	1547.818	4.736817	67.77056	4.877893	0.191481	1789.214	71.02527	3.10324	0.359291	**0.191481**
RT	1.303186	10.90342	5.374036	8.590222	54.33056	16.45637	5.18586	41.36147	8.450408	**0.277315**
FR	9.21875	5.15625	7.9375	3.71875	2.96875	9.15625	7.6875	4.875	2.75	**1.53125**

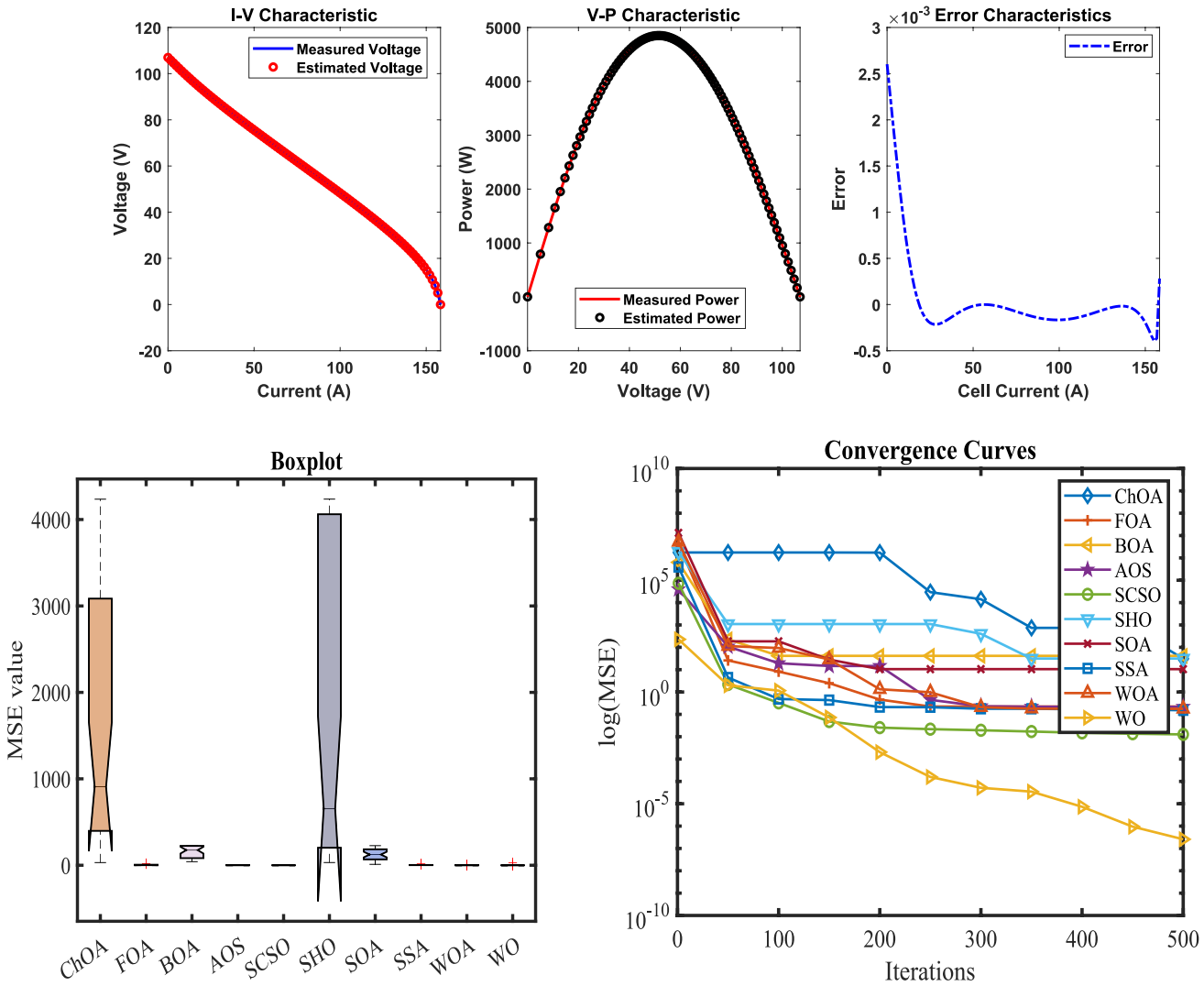

Fig. 4 Performance evaluation: **a** V-I, P-V, and error curves; **b** box plot of MSE; and **c** convergence curve

Precision tuning phase

While migration occurs under high risk, walrus herds tend to reproduce in currents where danger levels are low. The reproductive period is characterized by two main activities: onshore roosting and underwater foraging. The mathematical model describing this is:

Local refinement phase Our model classifies walrus population members into three groups: males, females, and juveniles. These different classifications each have their own specific approach to renewing their position.

Step 1, male walrus redistribution: Maintaining population diversity is essential for the algorithm's subsequent iterative search for optimal solutions. Inspired by the quasi-Monte Carlo method, which commonly uses the Halton sequence for generating well-distributed random sequences, we employ the Halton sequence distribution to update the positions of male walruses. This approach facilitates a broader spread of the population across the search space by evenly dividing the search area and selecting a random point within each division, ensuring both randomness and uniformity.
Step 2, female walrus position update: The position of a female walrus is updated based on the position of a male walrus ($Male^{t}_{i,j}$) and the position of the best-performing (lead) walrus ($Male^{t}_{i,j}$) Over the course of the algorithm's iterations, the influence of the male walrus on the female gradually decreases, while the influence of the lead walrus increases as shown in Eq. (25).

Table 4 Model parameters and performance metrics

Algorithm	ChOA	FOA	BOA	AOS	SCSO	SHO	SOA	SSA	WOA	WO
E_0(V)	1.157502	1.104249	1.031038	1.114312	1.118428	0.930544	1.2	1.086522	1.109847	1.113817
A(V)	0.273761	0.098002	0	0.151477	0.009086	0	0.056761	0.007716	0.140823	0.030383
$I_{0,c}$(mA.cm^{-2})	30	29.983	1.031038	25.54517	1.436924	0.80932	1.175941	10.47132	25.06851	5.468236
R_{ohm}(kΩ·cm^2)	0	0.002138	0	2.62E−05	0.004269	0.000212	0	0.004415	7.58E−07	0.003572
B(V)	0	0.081438	0.650038	0.143915	0.057794	0.468996	0.429495	0.057211	0.165816	0.069466
I_L(mA.cm^{-2})	200	160.1629	200	163.2878	159.6843	200	200	159.7134	165.3473	159.9381
$I_{0,a}$(mA.cm^{-2})	30	29.99203	18.77849	29.52441	1.96283	17.7709	12.8526	31.20439	28.28505	29.98569
Min	57.71668	0.081486	18.67755	0.42781	0.069386	38.00755	11.66502	0.451859	0.510524	**8.58E−06**
Max	**860,288.4**	13.9793	317.8949	8.61671	1.803293	1,569,043	317.8949	133.8987	2.325369	3.084046
Mean	28,599.03	4.259158	195.1047	1.719995	0.95846	51,892.34	170.8668	7.584448	1.527239	**0.343168**
Std	151,776.1	3.850005	102.7778	1.359664	0.555469	276,869.2	117.6631	23.19682	0.551924	**0.533209**
RT	0.436415	10.55872	5.455607	8.663967	71.78322	16.39041	7.124002	63.77852	8.567964	**0.401987**
FR	9.1875	4.71875	7.671875	3.75	2.78125	9.3125	7.734375	4.78125	3.75	**1.3125**

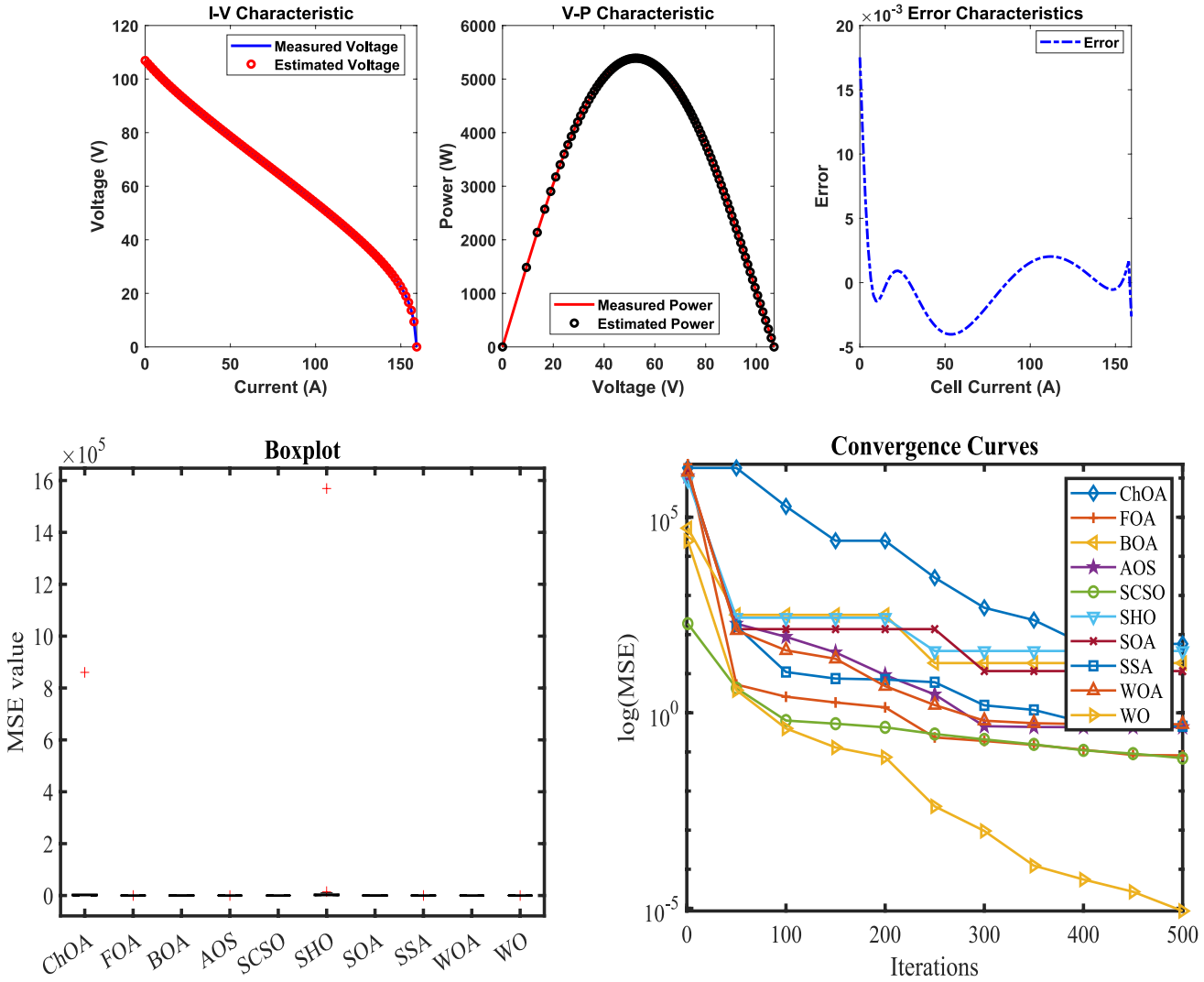

Fig. 5 Performance evaluation: **a** V-I, P-V, and error curves; **b** box plot of MSE; and **c** convergence curve

Table 5 Model parameters and performance metrics

Algorithm	ChOA	FOA	BOA	AOS	SCSO	SHO	SOA	SSA	WOA	WO
E_0(V)	1.2	1.114985	1.041827	1.110698	1.116668	1.101166	1.013237	1.095446	1.109007	1.113264
A(V)	0.183531	0.156522	0	0.141885	0.013337	0.029951	0	0.035833	0.126334	0.024353
$I_{0,c}$(mA.cm^{-2})	30	29.94422	0.469213	28.58207	2.560632	1.02272	0.529404	−87.9916	24.6979	4.274977
R_{ohm}(kΩ·cm^2)	1.47E−06	2.36E−05	0	0.000123	0.00344	0.002852	0	0.003426	2.29E−05	0.00311
B(V)	0.173202	0.102281	0.564359	0.117743	0.069552	0.000565	0.529036	0.077269	0.135528	0.074085
I_L(mA.cm^{-2})	200	160.2291	195.9488	160.948	159.9805	166.6867	194.6437	160.1153	161.7555	160.0317
$I_{0,a}$(mA.cm^{-2})	30	29.9566	6.213749	29.96209	4.214524	3.073456	17.83777	10.58883	26.46651	20.39292
Min	26.11171	0.592527	14.36627	0.402055	0.012839	64.42151	13.73095	0.177096	0.654642	**2.24E−06**
Max	5633.634	12.40877	442.1597	4.656191	3.141671	**9786.093**	442.1597	130.4338	4.471989	3.849704
Mean	1912.483	4.988781	214.7982	3.077271	0.962176	2153.669	251.1862	10.86783	2.991793	**0.362583**
Std	1976.614	3.535698	154.2135	1.233377	0.98608	2305.394	162.0464	22.25664	1.154924	**0.671162**
RT	0.507984	10.39658	5.673956	8.787967	54.41156	16.33662	5.251972	36.91263	8.798781	**0.286209**
FR	9.0625	4.625	7.859375	4.03125	2.1875	9.25	7.796875	4.875	4	**1.3125**

$$Female_{i,j}^{t+1} = Female_{i,j}^{t} + \alpha \bullet \left(Male_{i,j}^{t} - Female_{i,j}^{t}\right) + (1-\alpha) \bullet \left(X_{best}^{t} - Female_{i,j}^{t}\right) \tag{25}$$

In this equation, $Female_{i,j}^{t+1}$ denotes the new coordinate of the i-th female walrus along the j-th dimension at the next iteration. $Male_{i,j}^{t}$ and $Female_{i,j}^{t}$ coordinates of the i-th male and female walruses, respectively, in the j-th dimension.

Step 3, juvenile walrus position update: Due to their heightened risk of being targeted by killer whales and polar bears, particularly when located at the edge of the population, juvenile walruses must update their position to evade predation, as shown in Eqs. (26) and (27).

$$Juvenile_{i,j}^{t+1} = \left(O - Juvenile_{i,j}^{t}\right) \bullet P \tag{26}$$

$$O = X_{best}^{t} + Juvenile_{i,j}^{t} \bullet LF \tag{27}$$

In this equation, $Juvenile_{i,j}^{t+1}$ denotes the new coordinate of the i-th juvenile walrus along the j-th dimension at the next iteration. $Juvenile_{i,j}^{t}$ is its current coordinate in the same dimension. P represents the distress coefficient for juvenile walruses, a random value from the interval (0, 1). O signifies the reference safety position, and LF is a vector of random numbers following a Lévy distribution, modeling Lévy movement as shown in Eq. (28).

$$Levy(a) = 0.05 \times \frac{x}{|y|^{\frac{1}{a}}} \tag{28}$$

where x and y are two variables that follow a normal (Gaussian) distribution. Specifically, x is normally distributed with a mean of 0 and a variance of $\sigma^2 x$, and y is normally distributed with a mean of 0 and a variance of $\sigma^2 y$, as shown in Eq. (29).

$$\sigma_x = \left[\frac{\Gamma(1+\alpha)sin\left(\frac{\pi\alpha}{2}\right)}{\Gamma\left(\frac{1+\alpha}{2}\right)\alpha 2^{\frac{(\alpha-1)}{2}}}\right]^{\frac{1}{\alpha}}, \sigma_y = 1, \alpha = 1.5 \tag{29}$$

In this context, σ_x and σ_y denote the standard deviations, and the gamma function, $\Gamma(x)$, is equivalent to $(x+1)!$

Food acquisition strategies When animals forage underwater, they engage in both evasive maneuvers and food gathering.

Step 1, Escape behavior: Natural predators pose a threat to walruses during underwater foraging. Consequently, walruses will evacuate their immediate activity area upon receiving danger cues from conspecifics. This evasive behavior is observed in the late iteration of the WO, where a degree of population perturbation facilitates enhanced global exploratory capabilities for walruses, as shown in Eq. (30).

$$X_{i,j}^{t+1} = X_{i,j}^{t} \bullet R - \left|X_{best}^{t} - X_{i,j}^{t}\right| \bullet r_4^2 \tag{30}$$

In this context, $\left|X_{best}^{t} - X_{i,j}^{t}\right|$ signifies the distance from the current walrus to the best-performing walrus. r_4 is a random number uniformly distributed between 0 and 1.

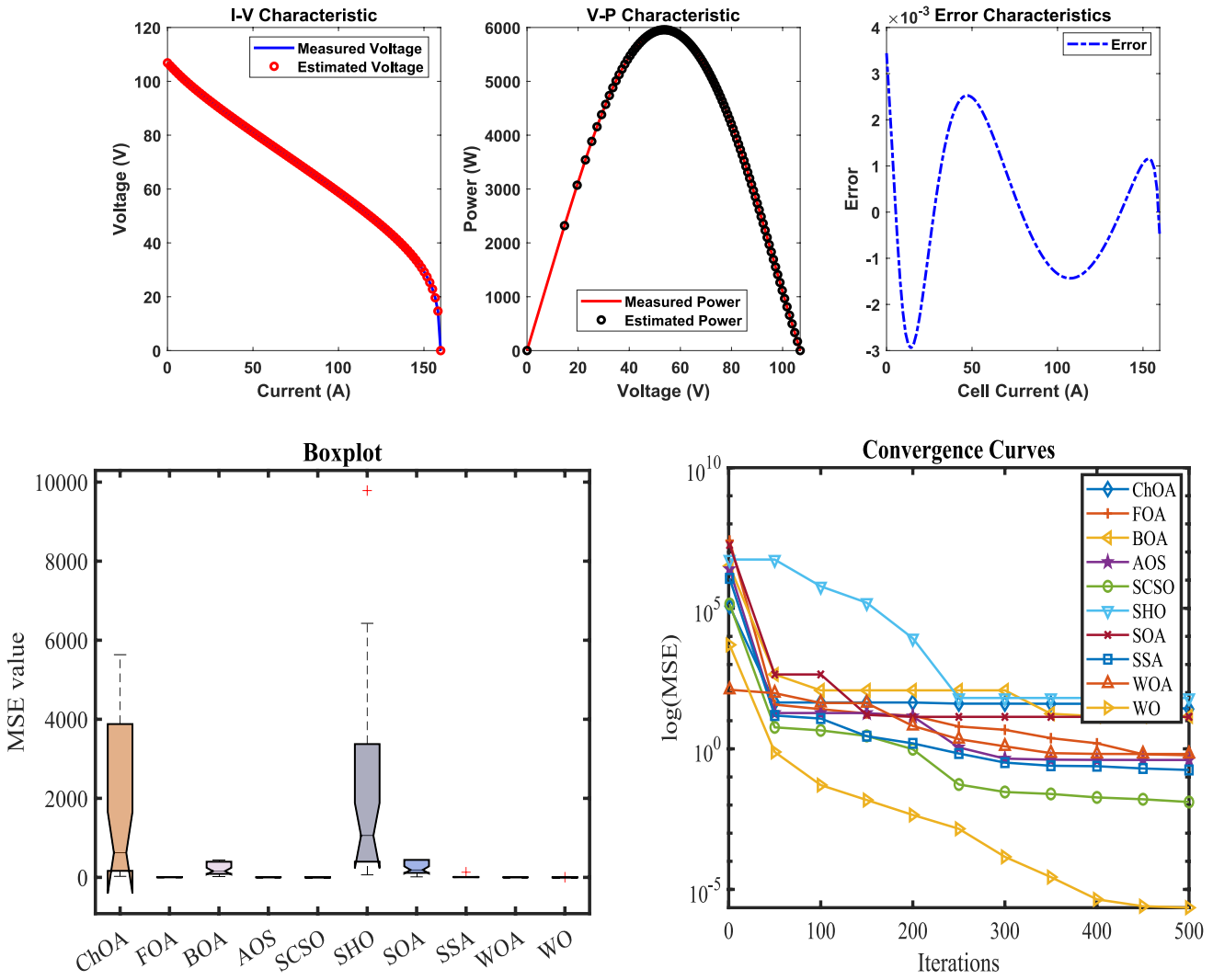

Fig. 6 Performance evaluation: **a** V-I, P-V, and error curves; **b** box plot of MSE; and **c** convergence curve

Table 6 Model parameters and performance metrics

Algorithm	ChOA	FOA	BOA	AOS	SCSO	SHO	SOA	SSA	WOA	WO
E_0(V)	1.2	1.116677	0.987037	1.109872	1.11442	1.2	0.996091	1.098828	1.107776	1.11224
A(V)	0.198349	0.147167	1.04E−06	0.138362	0.013216	0.1097	0	0.180789	0.131322	0.022779
$I_{0,c}$(mA.cm^{-2})	29.09871	28.56304	1.028062	28.55303	3.225097	30	0.607294	28.37913	27.31158	3.878272
R_{ohm}(kΩ·cm^2)	0	0	2.1E−05	5.61E−05	0.003124	0	0.000239	0.000393	1.65E−05	0.002813
B(V)	0.113213	0.100995	0.459898	0.108411	0.073838	0.4038	0.333925	0.102423	0.116727	0.078466
I_L(mA.cm^{-2})	200	160.3022	195.717	160.4536	160.06	200	170.8847	160.4174	160.6612	160.0998
$I_{0,a}$(mA.cm^{-2})	30	29.88016	8.128242	29.98685	3.34671	30	2.209133	110.9456	28.67429	17.27459
Min	28.23937	0.550456	16.89342	0.349998	0.012664	32.7111	20.34777	0.184528	0.400791	**7.39E−06**
Max	**57,887.11**	15.33215	517.2866	6.181232	3.06258	15,770.88	517.2866	129.7694	11.3449	4.39885
Mean	6696.388	6.568356	255.9843	3.297107	1.052802	2661.497	205.3203	11.17479	4.017428	**0.359477**
Std	12,547.06	3.493821	200.4767	1.947791	0.986612	3073.441	172.3354	22.24447	2.430789	**0.766815**
RT	0.49743	10.4671	5.421558	8.671926	53.895	16.40464	5.596275	53.28083	9.989626	**0.295862**
FR	9.21875	4.90625	7.84375	3.625	2.34375	9.15625	7.78125	4.8125	3.96875	**1.34375**

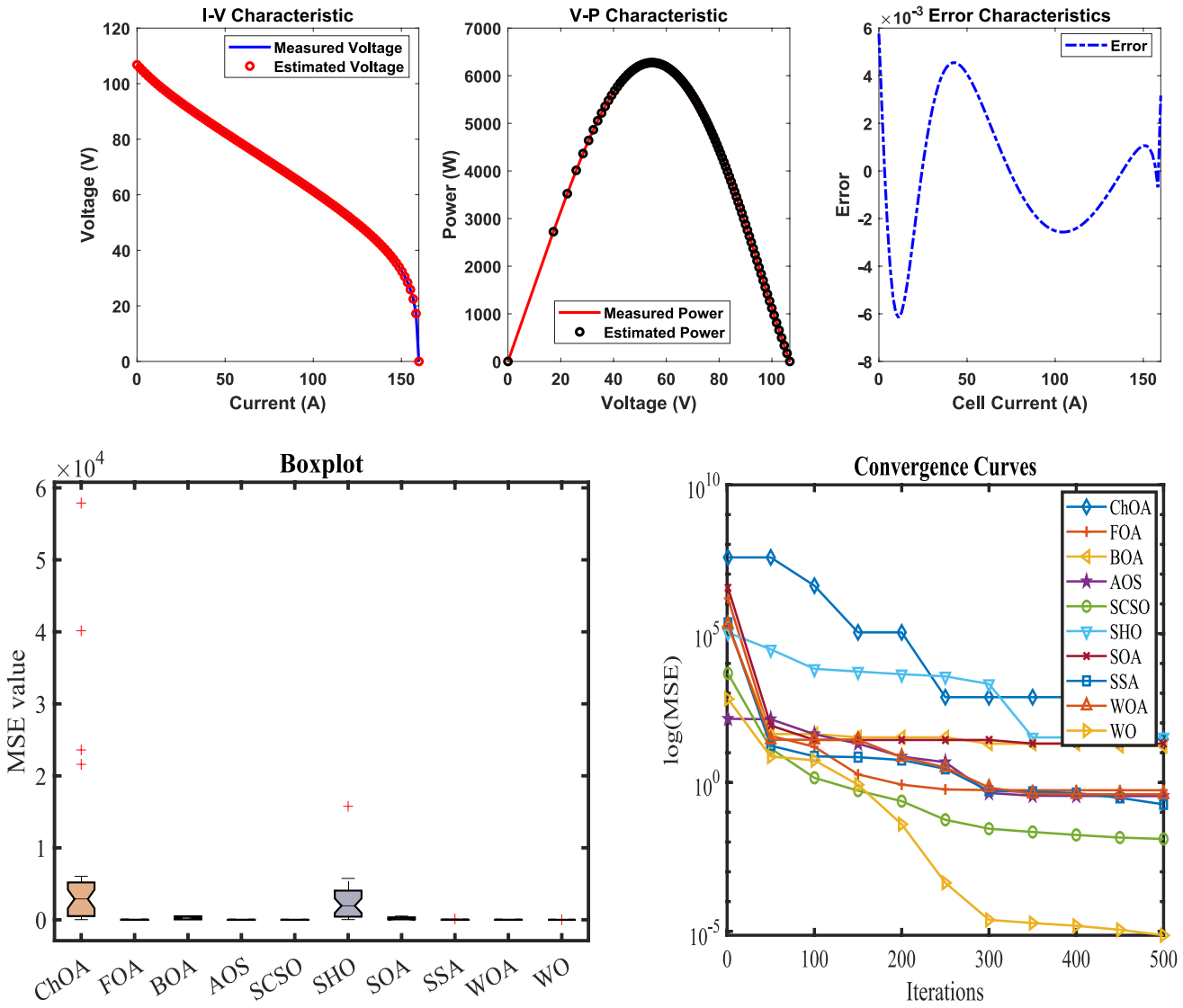

Fig. 7 Performance evaluation: **a** V-I, P-V, and error curves; **b** box plot of MSE; and **c** convergence curve

Table 7 Model parameters and performance metrics

Algorithm	ChOA	FOA	BOA	AOS	SCSO	SHO	SOA	SSA	WOA	WO
E_0(V)	1.2	1.088219	1.016516	1.109229	1.112472	1.144449	1.049592	1.124378	1.10095	1.111083
A(V)	0.126876	0.043334	0	0.119072	0.015304	0.132147	0	0.023048	0.121259	0.027887
$I_{0,c}$(mA.cm^{-2})	14.81541	29.2805	10.2164	23.27487	3.966709	23.03322	0.003809	1.318682	27.6735	4.20934
R_{ohm}(kΩ·cm^2)	6.37E−06	0.002402	0	9.51E−06	0.002721	4.63E−05	0	0.002288	2.77E−05	0.002425
B(V)	0.189765	0.075631	0.452042	0.113307	0.079611	0.185174	0.502234	0.093893	0.114965	0.082571
I_L(mA.cm^{-2})	200	160.0811	190.2151	160.4431	160.1104	199.9987	193.6549	160.258	160.4923	160.1302
$I_{0,a}$(mA.cm^{-2})	30	29.81267	15.57852	29.24592	4.006499	29.58251	23.07543	21.38848	29.35441	29.99431
Min	30.45907	0.231999	12.97844	0.378241	0.004683	19.61275	13.42378	0.178795	0.330831	**3.41E−05**
Max	**3,940,962**	23.28917	596.4659	9.462353	2.547822	27,334.69	596.4659	116.2901	7.735063	0.677027
Mean	125,638.1	7.072928	224.3523	4.201207	0.4902	2982.587	243.101	14.83364	4.505655	**0.17921**
Std	696,236.5	5.070622	220.6287	3.015033	0.644527	5052.768	219.2005	23.66061	2.256143	**0.177874**
RT	0.50961	12.62407	5.425773	8.816362	61.45491	20.26837	5.160462	36.87158	8.486899	**0.414119**
FR	9.09375	4.59375	7.890625	3.90625	1.96875	9.21875	7.734375	4.96875	4.1875	**1.4375**

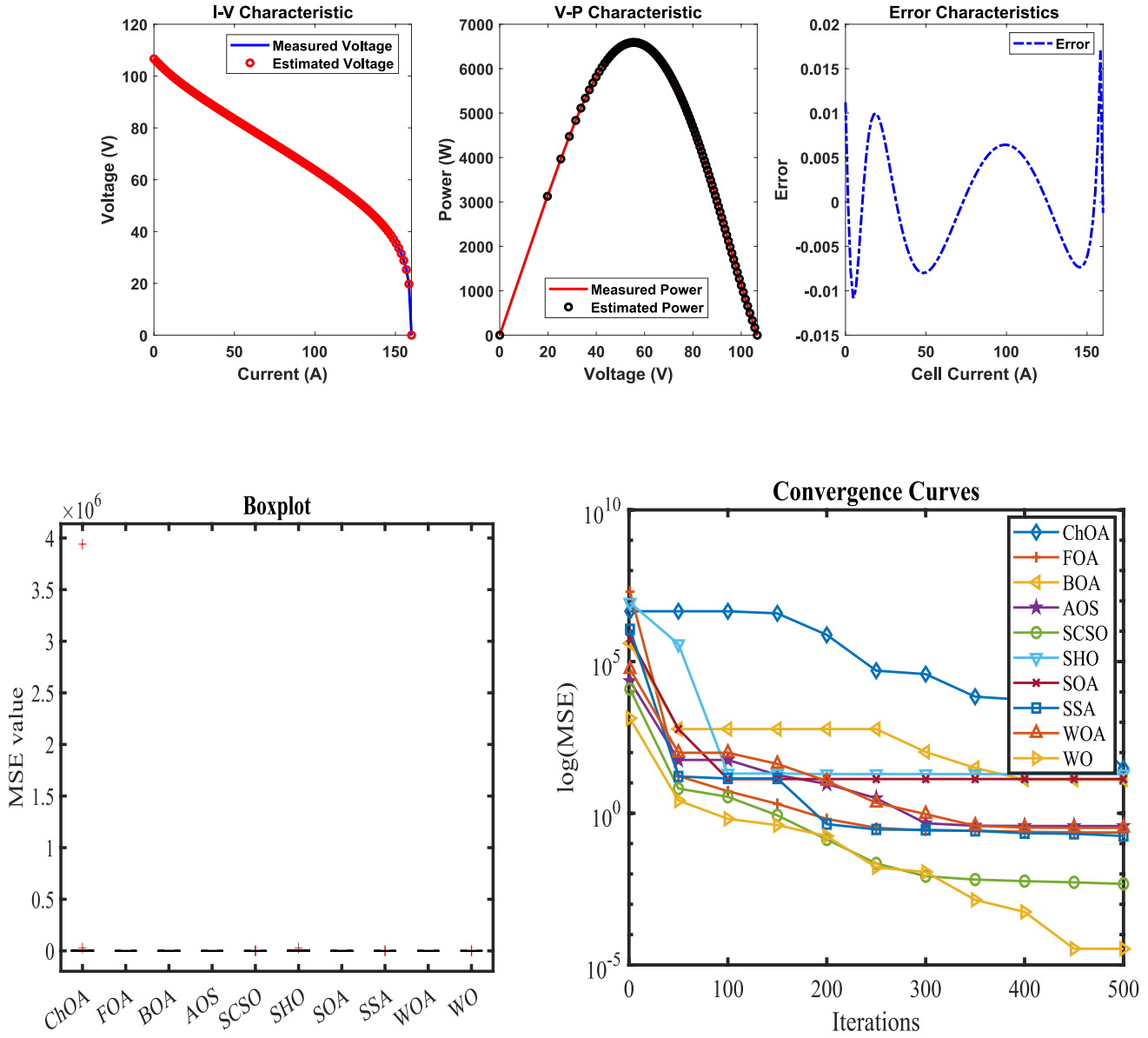

Fig. 8 Performance evaluation: **a** V-I, P-V, and error curves; **b** box plot of MSE; and **c** convergence curve

Step 2, collecting behavior: The walrus population benefits from a form of collective intelligence in foraging. Individuals move in response to their peers' locations, and by communicating these positions, the whole herd is better able to discover areas of high food abundance in the sea, as shown in Eqs. (31–34).

$$X_{i,j}^{t+1} = \left(X_1 + X_2\right)/2 \tag{31}$$

$$\begin{cases} X_1 = X_{best}^t - a_1 \times b_1 \times \left|X_{best}^t - X_{i,j}^t\right| \\ X_2 = X_{Second}^t - a_2 \times b_2 \times \left|X_{Second}^t - X_{i,j}^t\right| \end{cases} \tag{32}$$

$$a = \beta \times r_5 - \beta \tag{33}$$

$$b = tan(\theta) \tag{34}$$

The gathering behavior of a walrus is shaped by two weights, X1 and X2. X_{Second}^t is the second walrus's current position, and $\left|X_{Second}^t - X_{i,j}^t\right|$ calculates the distance between the current walrus and the second walrus. a and b serve as gathering coefficients, r5 is a random number between 0 and 1, and θ varies from 0 to π.

The WO methodology The walrus optimization (WO) algorithm's progression, specifically its shift between exploration

Table 8 Model parameters and performance metrics

Algorithm	ChOA	FOA	BOA	AOS	SCSO	SHO	SOA	SSA	WOA	WO
E_0(V)	0.95894	1.075659	1.0335	1.079196	1.076336	1.048506	1.040081	1.056202	1.083323	1.085504
A(V)	0.006917	0.141859	0	0.13943	0.112229	0.014133	0	0.624963	0.147008	0.024648
$I_{0,c}$(mA.cm^{-2})	18.90748	29.97177	9.106059	28.1721	29.99957	30	9.325348	85.11258	29.48083	4.28987
R_{ohm}(kΩ·cm^2)	0	0	0	4.81E−06	0.001091	0	0	−0.00137	4.17E−05	0.003106
B(V)	0.394056	0.128162	0.624602	0.129059	0.097042	0.633544	0.532755	0.085279	0.116964	0.074171
I_L(mA.cm^{-2})	200	161.6082	200	161.7285	160.4778	200	187.8673	160.2999	161.0573	160.0332
$I_{0,a}$(mA.cm^{-2})	30	29.97213	9.898402	29.60389	29.99958	30	12.86008	177.3796	29.74665	21.37068
Min	61.91624	0.406856	19.823	0.41139	0.135886	35.43164	24.34716	0.418989	0.346578	**2.04E−07**
Max	**22,747.73**	35.07304	402.8676	5.128774	2.389011	815,614.6	402.8676	55.43841	3.821846	2.128707
Mean	2650.987	6.123438	200.723	2.292947	1.139843	29,214.76	206.683	7.323359	2.484671	**0.339518**
Std	5297.107	6.05472	141.5331	1.149432	0.741014	143,831.5	144.3029	10.56751	1.011117	**0.37716**
RT	0.486651	10.56574	11.51553	9.60654	57.63881	14.73009	6.148294	36.25813	7.739879	**0.234275**
FR	9.25	5.15625	7.796875	3.65625	2.28125	9.15625	7.734375	4.65625	3.96875	**1.34375**

and exploitation, is governed by a danger signal. When this signal's absolute value is at least 1, the walrus population relocates to a new area within the solution space, characteristic of the algorithm's early exploration phase. However, if the danger signal is less than 1, the population undergoes reproduction, representing the algorithm's later exploitation phase. Within this exploitation phase, a security signal becomes critical, determining if individual walruses rest or seek food. Notably, foraging involves two behaviors: gathering and fleeing, both of which are regulated by danger signals. Figure 3 provides a comprehensive illustration of the WO's flowchart.

Results and discussion

Analysis of results

Researchers used the walrus optimization (WO) algorithm, implemented in MATLAB 2021a on a Windows Server 2019 system (Intel Core i7-11700 k 3.6 GHz, 32 GB RAM), to optimize parameters for various experimentally validated mathematical models of SOFC data. The primary goal was to minimize the mean squared error (MSE) between measured and predicted voltage values.

To assess its effectiveness, WO was rigorously compared against nine well-known metaheuristic algorithms: Chimp Optimization Algorithm (ChOA) [58], Following Optimization Algorithm (FOA) [59], Butterfly Optimization Algorithm (BOA) [60], Atomic Orbital Search (AOS) [61], Sand Cat Swarm Optimization (SCSO) [62], Spotted Hyena Optimization (SHO) [63], Seagull Optimization Algorithm (SOA) [64], Salp Swarm Algorithm (SSA) [65], and Whale Optimization Algorithm (WOA) [66]. For statistical validity, each algorithm ran 40 times with 50 individuals and a maximum of 500 iterations.

The experimental data used for the validation of the model in this study is based on the available literature data, which provide detailed information on the operational characteristics of solid oxide fuel cells (SOFCs) under different conditions. The particular configurations, such as the electrode and electrolyte materials and the dimensions of the SOFC assembly, are the same as those in widely cited experimental works, especially those of a 96-cell dynamic tubular stack. The anode is usually a nickel-yttria-stabilized zirconia (Ni-YSZ) cermet, the cathode is commonly lanthanum strontium manganite (LSM), and the electrolyte is yttria-stabilized zirconia (YSZ). The geometric parameters, including active surface area and cell thickness, match typical industrial and research setups for such stacks, ensuring the relevance and applicability of the model to real-world systems. This following of documented experimental setups gives a strong basis for the parameter identification process and the following validation of the proposed optimization methodology.

The study evaluated WO's convergence, error distribution, and stability across different SOFC models using I–V and P-V curves, box plots, and convergence curves. Friedman ranking tests confirmed WO's statistically superior performance, showcasing its effectiveness, computational efficiency, and robustness in optimizing SOFC parameters. Additionally, a dynamic tubular SOFC model was simulated under the operating conditions detailed in Table 1 (temperature, pressure, flow rates, load current). Seven critical SOFC parameters were estimated, with their physical constraints outlined in Table 2.

Fuel cell sheet 1

To accurately model SOFC electrochemical behavior at 1073 K, the walrus optimization (WO) algorithm was deployed to determine seven critical parameters. This optimization aimed

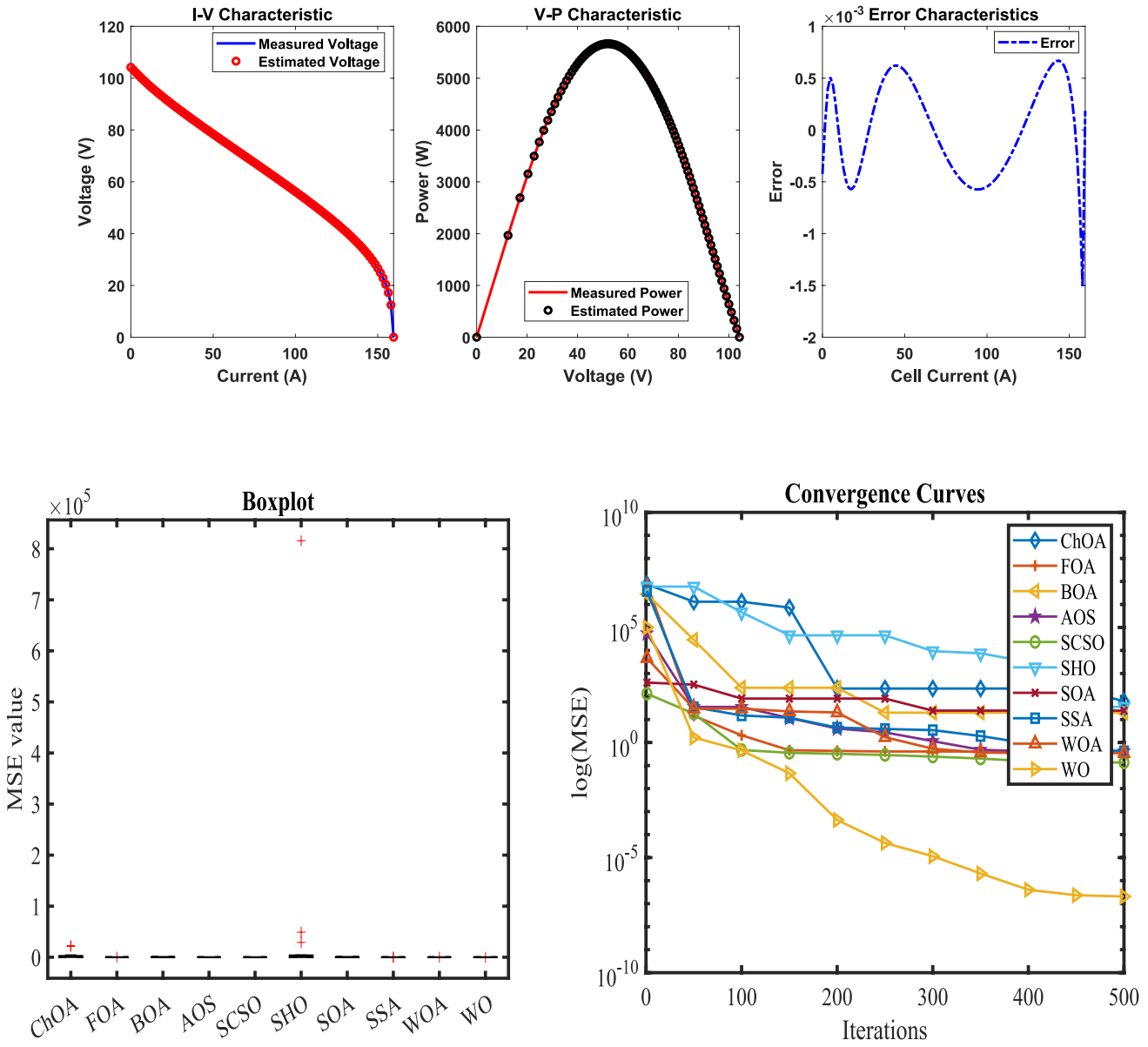

Fig. 9 Performance evaluation: **a** V-I, P-V, and error curves; **b** box plot of MSE; and **c** convergence curve

to reduce the mean squared error (MSE) between model predictions and actual experimental voltage–current (V-I) data.

The results, summarized in Table 3, clearly establish WO's superiority over nine competing algorithms. WO achieved the best performance metrics, including the lowest minimum MSE (2.57E−07), highest stability (standard deviation, 0.191481), fastest execution time (0.277315 s), and the top Friedman ranking test score (1.53125).

Further graphical validation confirmed WO's exceptional predictive accuracy. Figure 4a illustrates how closely WO's V-I and P-V curves align with simulated data, precisely capturing the electrical performance and maximum power point. Error analysis reinforced its high precision, with nearly all voltage prediction errors within a tight ± 0.05 V range. The rapid and consistent decrease in MSE towards the optimal solution, shown in Fig. 4b, demonstrates WO's efficient convergence. Finally, Fig. 4c, showcasing 100 independent runs, powerfully illustrates WO's remarkable robustness through its narrowest interquartile range, lowest median MSE, and absence of significant outliers, ensuring reliable and consistent performance.

Fuel cell sheet 2

To accurately model SOFC electrochemical behavior at 1123 K, the walrus optimization (WO) algorithm was deployed to

Table 9 Model parameters and performance metrics

Algorithm	ChOA	FOA	BOA	AOS	SCSO	SHO	SOA	SSA	WOA	WO
E_0(V)	0.919919	1.095627	0.995063	1.109551	1.11244	1.085459	0.967204	1.10424	1.112449	1.113391
A(V)	0.014957	0.035254	0	0.135087	0.0193	0	0	0.008006	0.145539	0.026123
$I_{0,c}$(mA.cm^{-2})	30	28.99332	2.46526	24.98241	5.122358	15.36177	14.16651	0.43251	27.80408	4.38669
R_{ohm}(kΩ·cm^2)	8.33E−08	0.00344	0	1.04E−05	0.003214	7.52E−16	0	0.003624	1.8E−05	0.003086
B(V)	0.416837	0.053502	0.509518	0.128142	0.073342	0.645578	0.428434	0.071676	0.11633	0.074089
I_L(mA.cm^{-2})	200	159.8333	196.4124	161.378	160.0238	200	191.4391	160.0398	160.8298	160.0316
$I_{0,a}$(mA.cm^{-2})	30	29.86612	3.65737	29.77281	8.185323	30	24.22506	23.13488	29.64176	25.44792
Min	55.4642	0.46924	14.52288	0.542154	0.000483	26.11451	24.98058	0.293496	0.435479	**9.79E−06**
Max	**5081.396**	30.23994	442.1597	4.586806	2.696976	26,640.45	442.1597	123.7361	4.669444	1.250367
Mean	1500.191	6.757497	195.5933	3.334809	0.921034	3612.557	228.82	10.58471	2.714423	**0.269078**
Std	1904.502	6.306621	158.7363	1.128935	0.951839	4690.98	162.1822	21.05284	1.396584	**0.259588**
RT	0.409812	9.426051	5.003052	8.244726	42.6553	14.66732	3.966137	28.75217	6.666429	**0.20451**
FR	9.03125	4.75	7.671875	4.15625	2.0625	9.3125	7.921875	5.0625	3.59375	**1.4375**

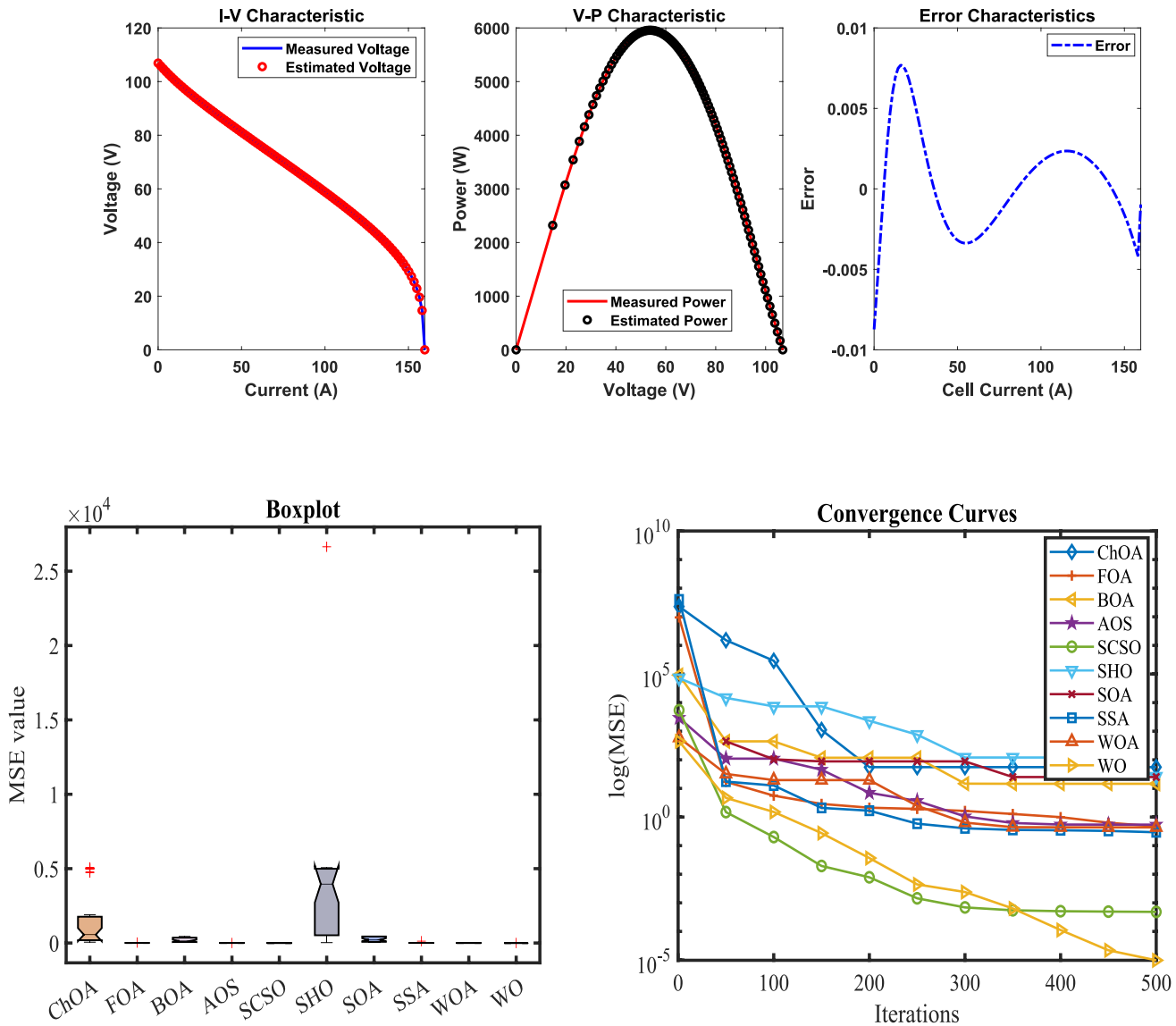

Fig. 10 Performance evaluation: **a** V-I, P-V, and error curves; **b** box plot of MSE; and **c** convergence curve

Table 10 Model parameters and performance metrics

Algorithm	ChOA	FOA	BOA	AOS	SCSO	SHO	SOA	SSA	WOA	WO
E_0(V)	1.2	1.123389	1.023293	1.125107	1.11998	1.085448	1.033637	1.112666	1.119028	1.125991
A(V)	4.67E−08	0.150603	0	0.132609	0.034903	0.088828	0	0.013533	0.132382	0.027832
$I_{0,c}$(mA.cm^{-2})	2.225812	30	4.898427	25.50351	12.96065	30	0.641535	5.130368	26.6612	4.691924
R_{ohm}(kΩ·cm^2)	0.003611	1.26E−07	0	5.43E−05	0.002761	0.001676	0	0.00339	0.000133	0.003059
B(V)	0.307492	0.114055	0.381629	0.123664	0.079047	0.168555	0.529604	0.074215	0.127409	0.074328
I_L(mA.cm^{-2})	200	160.6858	170.5794	161.0121	160.0874	200	200	160.0558	161.3061	160.0354
$I_{0,a}$(mA.cm^{-2})	29.99999	30	7.820897	26.80503	14.22143	30	19.44944	9.01656	29.9714	29.6656
Min	39.98254	0.413321	30.30312	0.569806	0.023629	22.28075	13.95536	0.11297	0.570679	**1.09E−05**
Max	**35,525.51**	13.10177	464.6382	5.290752	3.057418	851,522.9	464.6382	12.32244	4.808453	0.935937
Mean	3609.245	5.518929	219.877	3.309124	1.220552	30,026.03	232.4627	5.645151	3.007102	**0.202254**
Std	6283.812	3.453983	166.1637	1.328689	0.966286	150,041.6	180.6218	4.741673	1.429485	**0.227151**
RT	0.42012	8.3115	4.32098	6.836154	42.66844	12.40907	4.048607	29.27524	6.740178	**0.20175**
FR	9.25	4.9375	7.875	4.03125	2.59375	9.140625	7.734375	4.40625	3.90625	**1.125**

determine seven critical parameters. This optimization aimed to reduce the mean squared error (MSE) between model predictions and actual experimental voltage–current (V-I) data.

The results, summarized in Table 4, clearly establish WO's superiority over nine competing algorithms. WO achieved the best performance metrics, including the lowest minimum MSE (8.58E−06), highest stability (standard deviation, 0.533209), fastest execution time (0.401987 s), and the top Friedman ranking test score (1.3125).

Further graphical validation confirmed WO's exceptional predictive accuracy. Figure 5a illustrates how closely WO's V-I and P-V curves align with simulated data, precisely capturing the electrical performance and maximum power point. Error analysis reinforced its high precision, with nearly all voltage prediction errors within a tight ± 0.05 V range. The rapid and consistent decrease in MSE towards the optimal solution, shown in Fig. 5b, demonstrates WO's efficient convergence. Finally, Fig. 5c, showcasing 100 independent runs, powerfully illustrates WO's remarkable robustness through its narrowest interquartile range, lowest median MSE, and absence of significant outliers, ensuring reliable and consistent performance.

Fuel cell sheet 3

To accurately model SOFC electrochemical behavior at 1173 K, the walrus optimization (WO) algorithm was deployed to determine seven critical parameters. This optimization aimed to reduce the mean squared error (MSE) between model predictions and actual experimental voltage–current (V-I) data.

The results, summarized in Table 5, clearly establish WO's superiority over nine competing algorithms. WO achieved the best performance metrics, including the lowest minimum MSE (2.24E−06), highest stability (standard deviation, 0.671162), fastest execution time (0.286209 s), and the top Friedman ranking test score (1.3125).

Further graphical validation confirmed WO's exceptional predictive accuracy. Figure 6a illustrates how closely WO's V-I and P-V curves align with simulated data, precisely capturing the electrical performance and maximum power point. Error analysis reinforced its high precision, with nearly all voltage prediction errors within a tight ± 0.05 V range. The rapid and consistent decrease in MSE towards the optimal solution, shown in Fig. 6b, demonstrates WO's efficient convergence. Finally, Fig. 6c, showcasing 100 independent runs, powerfully illustrates WO's remarkable robustness through its narrowest interquartile range, lowest median MSE, and absence of significant outliers, ensuring reliable and consistent performance.

Fuel cell sheet 4

To accurately model SOFC electrochemical behavior at 1223 K, the walrus optimization (WO) algorithm was deployed to determine seven critical parameters. This optimization aimed to reduce the mean squared error (MSE) between model predictions and actual experimental voltage–current (V-I) data.

The results, summarized in Table 6, clearly establish WO's superiority over nine competing algorithms. WO achieved the best performance metrics, including the lowest minimum MSE (7.39E−06), highest stability (standard deviation, 0.766815), fastest execution time (0.295862 s), and the top Friedman ranking test score (1.34375).

Further graphical validation confirmed WO's exceptional predictive accuracy. Figure 7a illustrates how closely WO's V-I and P-V curves align with simulated data, precisely capturing the electrical performance and maximum power point. Error analysis reinforced its high precision, with nearly all voltage prediction errors within a tight ± 0.05 V range. The rapid and consistent decrease in MSE towards the optimal solution, shown in Fig. 7b, demonstrates WO's efficient

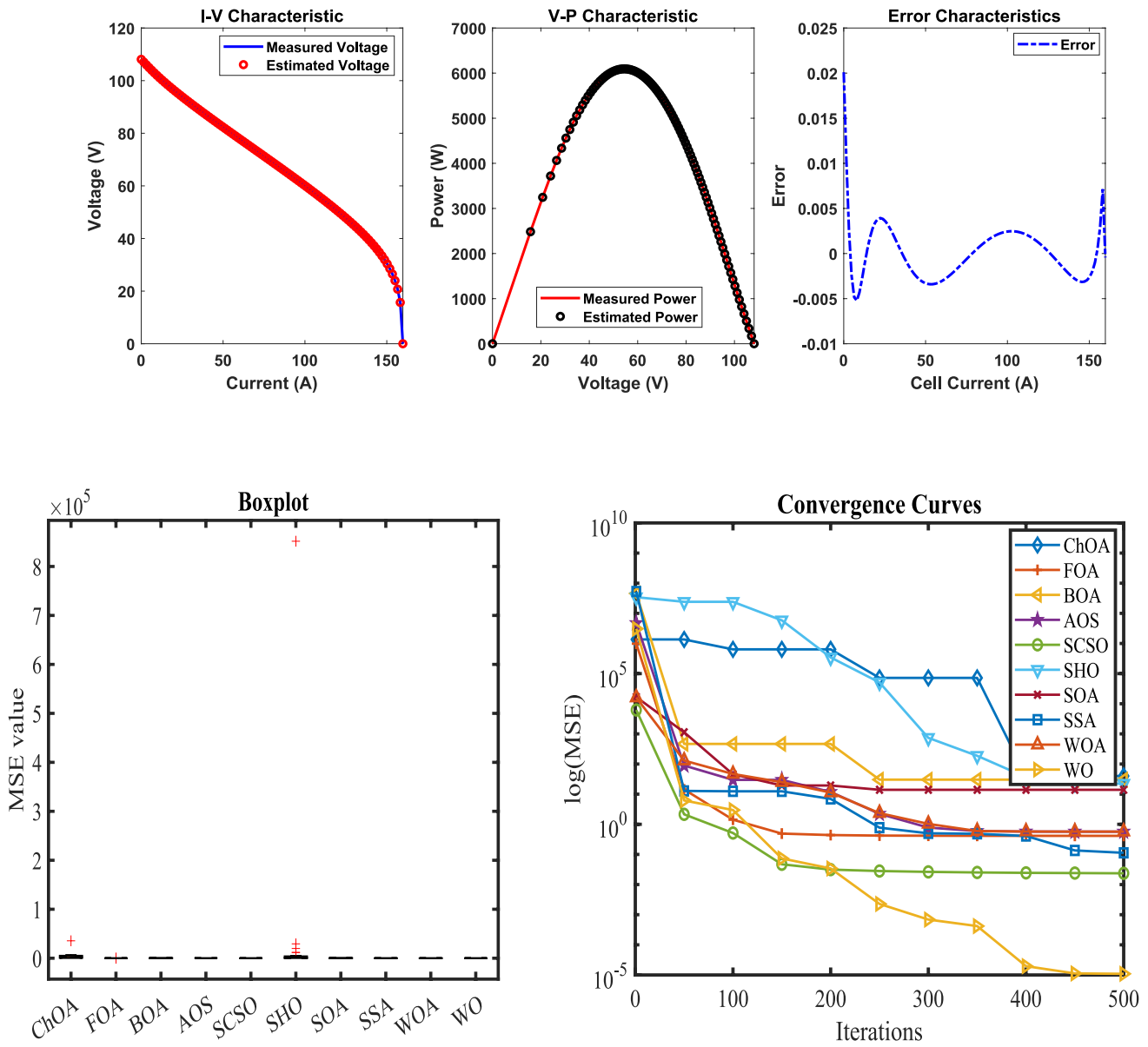

Fig. 11 Performance evaluation **a** V-I, P-V, and error curves; **b** box plot of MSE; and **c** convergence curve

convergence. Finally, Fig. 7c, showcasing 100 independent runs, powerfully illustrates WO's remarkable robustness through its narrowest interquartile range, lowest median MSE, and absence of significant outliers, ensuring reliable and consistent performance.

Fuel cell sheet 5

To accurately model SOFC electrochemical behavior at 1273 K, the walrus optimization (WO) algorithm was deployed to determine seven critical parameters. This optimization aimed to reduce the mean squared error (MSE) between model predictions and actual experimental voltage–current (V–I) data.

The results, summarized in Table 7, clearly establish WO's superiority over nine competing algorithms. WO achieved the best performance metrics, including the lowest minimum MSE (3.41E−05), highest stability (standard deviation, 0.177874), fastest execution time (0.414119 s), and the top Friedman ranking test score (1.4375).

Further graphical validation confirmed WO's exceptional predictive accuracy. Figure 8a illustrates how closely WO's V-I and P-V curves align with simulated data, precisely capturing the electrical performance and maximum power point. Error analysis reinforced its high precision, with nearly all

voltage prediction errors within a tight ± 0.05 V range. The rapid and consistent decrease in MSE towards the optimal solution, shown in Fig. 8b, demonstrates WO's efficient convergence. Finally, Fig. 8c, showcasing 100 independent runs, powerfully illustrates WO's remarkable robustness through its narrowest interquartile range, lowest median MSE, and absence of significant outliers, ensuring reliable and consistent performance.

Fuel cell sheet 6

To accurately model SOFC electrochemical behavior at 1 atm, the walrus optimization (WO) algorithm was deployed to determine seven critical parameters. This optimization aimed to reduce the Mean Squared Error (MSE) between model predictions and actual experimental voltage–current (V-I) data.

The results, summarized in Table 8, clearly establish WO's superiority over nine competing algorithms. WO achieved the best performance metrics, including the lowest minimum MSE (2.04E−07), highest stability (standard deviation, 0.37716), fastest execution time (0.234275 s), and the top Friedman ranking test score (1.34375).

Further graphical validation confirmed WO's exceptional predictive accuracy. Figure 9a illustrates how closely WO's V-I and P-V curves align with simulated data, precisely capturing the electrical performance and maximum power point. Error analysis reinforced its high precision, with nearly all voltage prediction errors within a tight ± 0.05 V range. The rapid and consistent decrease in MSE towards the optimal solution, shown in Fig. 9b, demonstrates WO's efficient convergence. Finally, Fig. 9c, showcasing 100 independent runs, powerfully illustrates WO's remarkable robustness through its narrowest interquartile range, lowest median MSE, and absence of significant outliers, ensuring reliable and consistent performance.

Fuel cell sheet 7

To accurately model SOFC electrochemical behavior at 3 atm, the walrus optimization (WO) algorithm was deployed to determine seven critical parameters. This optimization aimed to reduce the Mean Squared Error (MSE) between model predictions and actual experimental voltage–current (V-I) data.

The results, summarized in Table 9, clearly establish WO's superiority over nine competing algorithms. WO achieved the best performance metrics, including the lowest minimum MSE (9.79E−06), highest stability (standard deviation, 0.259588), fastest execution time (0.20451 s), and the top Friedman ranking test score (1.4375).

Further graphical validation confirmed WO's exceptional predictive accuracy. Figure 10a illustrates how closely WO's V-I and P-V curves align with simulated data, precisely capturing the electrical performance and maximum power point. Error analysis reinforced its high precision, with nearly all voltage prediction errors within a tight ± 0.05 V range. The rapid and consistent decrease in MSE towards the optimal solution, shown in Fig. 10b, demonstrates WO's efficient convergence. Finally, Fig. 10c, showcasing 100 independent runs, powerfully illustrates WO's remarkable robustness through its narrowest interquartile range, lowest median MSE, and absence of significant outliers, ensuring reliable and consistent performance.

Fuel cell sheet 8

To accurately model SOFC electrochemical behavior at 5 atm, the walrus optimization (WO) algorithm was deployed to determine seven critical parameters. This optimization aimed to reduce the Mean Squared Error (MSE) between model predictions and actual experimental voltage–current (V-I) data.

Table 11 Model parameters and performance metrics

Algorithm	ChOA	FOA	BOA	AOS	SCSO	SHO	SOA	SSA	WOA	WO
E_0(V)	1.078318	1.129079	1.065327	1.138041	1.134574	1.2	1.021126	1.122362	1.130457	1.134751
A(V)	4.02E−08	0.084779	0	0.131891	0.018806	0.002422	0	0.15176	0.144659	0.023513
$I_{0,c}$(mA.cm^{-2})	30	22.99148	2.206802	21.97384	4.602763	30	0.486259	−210.473	29.58511	4.155141
R_{ohm}(kΩ·cm^2)	5.48E−06	0.0015	0	3.46E−05	0.003225	0.004815	0	0.00212	7.78E−05	0.003127
B(V)	0.639475	0.094929	0.517886	0.123051	0.073455	0.000555	0.533839	0.0933	0.117053	0.074038
I_L(mA.cm^{-2})	200	160.3038	188.9708	160.9109	160.0286	200	200	160.295	160.7824	160.033
$I_{0,a}$(mA.cm^{-2})	30	24.66251	15.32162	28.86902	8.115176	30	1.109947	24.94113	29.87549	18.77978
Min	27.52029	0.160293	17.31602	0.655987	0.000551	101.4838	14.19011	0.139917	0.43817	**7.19E−06**
Max	**87,263.12**	20.25943	481.335	13.25718	3.047818	9105.411	481.335	26.9087	7.599598	3.824232
Mean	4651.25	6.356443	173.2221	3.71298	1.331021	2566.382	249.3063	7.010931	3.541167	**0.391688**
Std	15,214.93	4.695745	153.8329	2.276751	1.17765	2296.819	202.0979	5.699598	1.514132	**0.649256**
RT	0.368707	8.181957	4.187557	6.829829	47.61055	17.57831	5.436887	36.65934	8.321777	**0.265131**
FR	9.28125	4.65625	7.640625	4	2.21875	9.3125	7.765625	4.75	3.9375	**1.4375**

The results, summarized in Table 10, clearly establish WO's superiority over nine competing algorithms. WO achieved the best performance metrics, including the lowest minimum MSE (1.09E−05), highest stability (standard deviation, 0.227151), fastest execution time (0.20175 s), and the top Friedman ranking test score (1.125).

Further graphical validation confirmed WO's exceptional predictive accuracy. Figure 11a illustrates how closely WO's V-I and P-V curves align with simulated data, precisely capturing the electrical performance and maximum power point. Error analysis reinforced its high precision, with nearly all voltage prediction errors within a tight ± 0.05 V range. The rapid and consistent decrease in MSE towards the optimal solution, shown in Fig. 11b, demonstrates WO's efficient convergence. Finally, Fig. 11c, showcasing 100 independent runs, powerfully illustrates WO's remarkable robustness through its narrowest interquartile range, lowest median MSE, and absence of significant outliers, ensuring reliable and consistent performance.

Fuel cell sheet 9

To accurately model SOFC electrochemical behavior at 7 atm, the walrus optimization (WO) algorithm was deployed to determine seven critical parameters. This optimization aimed to reduce the Mean Squared Error (MSE) between model predictions and actual experimental voltage–current (V-I) data.

The results, summarized in Table 11, clearly establish WO's superiority over nine competing algorithms. WO achieved the best performance metrics, including the lowest minimum MSE (7.19E−06), highest stability (standard

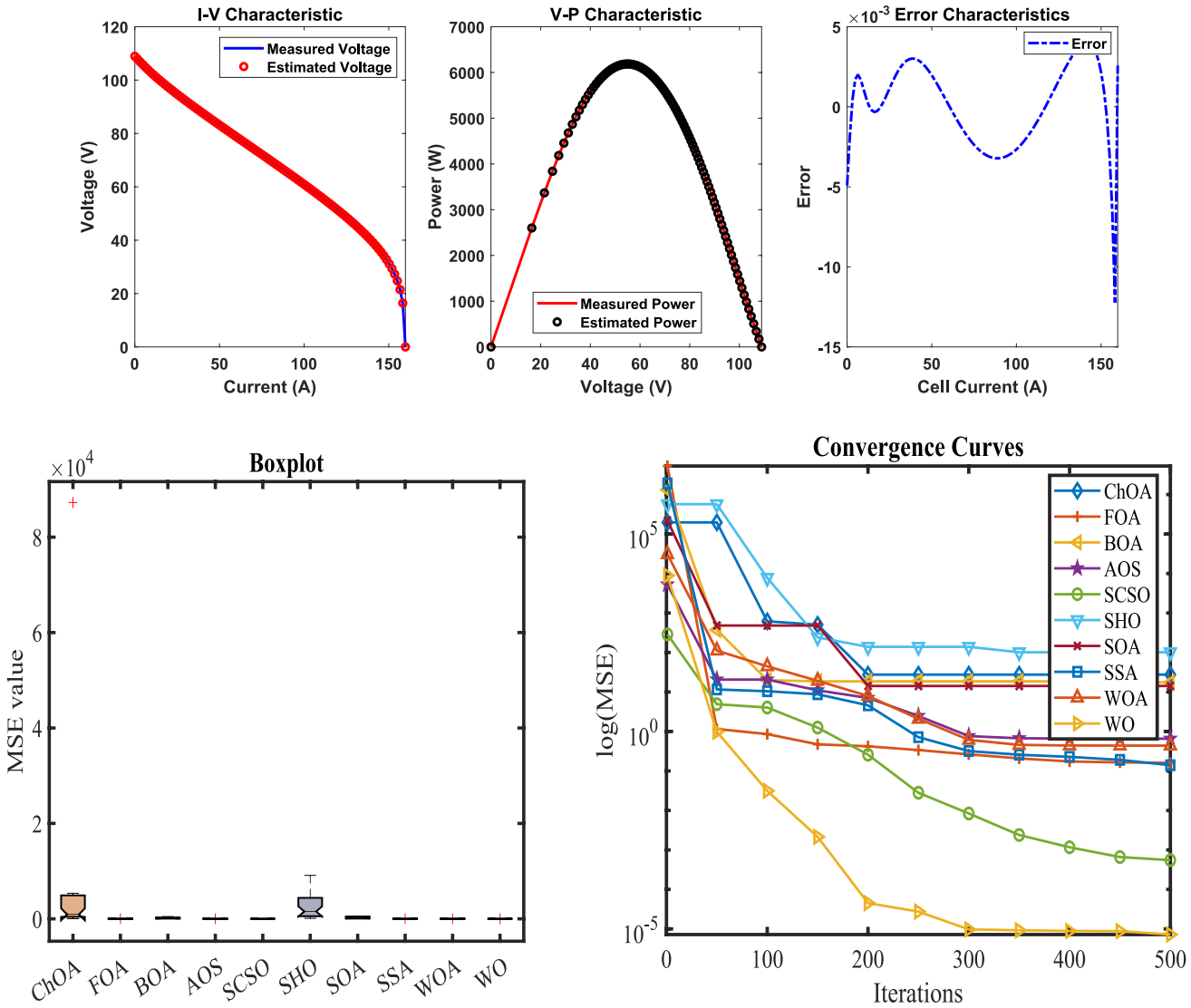

Fig. 12 Performance evaluation: **a** V-I, P-V, and error curves; **b** box plot of MSE; and **c** convergence curve

Table 12 Model parameters and performance metrics

Algorithm	ChOA	FOA	BOA	AOS	SCSO	SHO	SOA	SSA	WOA	WO
E_0(V)	0.987899	1.128964	1.086889	1.140834	1.144268	1.041099	1.06264	1.1481	1.142815	1.140687
A(V)	0.087287	0.088999	0	0.117325	0.028154	0.066778	0	0.005795	0.136047	0.02825
$I_{0,c}$(mA.cm^{-2})	27.22755	29.66193	1.593436	21.0868	4.144196	27.68928	1.18673	0.033634	23.45835	4.829221
R_{ohm}(kΩ·cm^2)	0	0.001778	0	0.000138	0.002946	2.16E−13	0	0.003591	4.4E−05	0.003049
B(V)	0.171085	0.084326	0.546128	0.130661	0.078209	0.295878	0.588024	0.074952	0.121026	0.074439
I_L(mA.cm^{-2})	200	160.1278	188.5377	161.1895	160.0778	200	200	160.0759	160.8337	160.0365
$I_{0,a}$(mA.cm^{-2})	30	29.97054	5.356498	25.12267	24.04581	30	1.216507	1.439352	29.97837	29.99809
Min	79.6889	0.087781	23.88065	0.795776	0.012571	31.28964	14.55786	0.32341	0.599578	**3.98E−05**
Max	**23,387.74**	16.23921	494.773	5.827194	3.499736	201,338	494.773	13.97564	5.617196	3.665909
Mean	3621.531	5.940988	207.8727	3.378079	1.258158	9391.96	226.7469	8.676507	3.646973	**0.613548**
Std	4285.653	4.288008	162.0842	1.567283	1.171597	35,171.29	195.577	4.352334	1.515289	**0.934517**
RT	0.490645	10.47629	5.574455	8.67113	55.23288	15.90467	5.399242	38.11086	8.520243	**0.320533**
FR	9.34375	4.40625	7.78125	3.84375	2.0625	9.125	7.75	5.28125	3.84375	**1.5625**

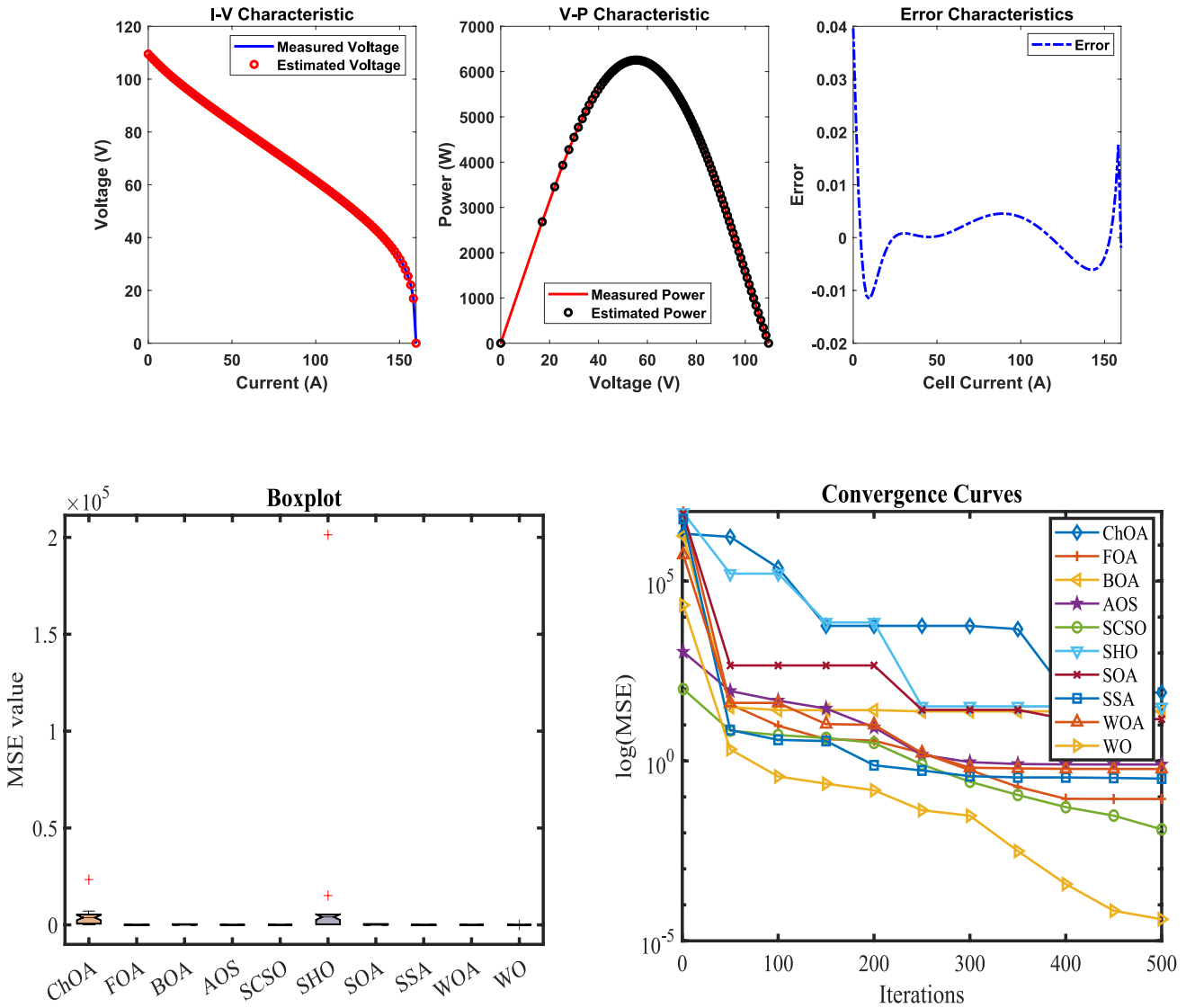

Fig. 13 Performance evaluation: **a** V-I, P-V, and error curves; **b** box plot of MSE; and **c** convergence curve

deviation, 0.649256), fastest execution time (0.265131 s), and the top Friedman ranking test score (1.4375).

Further graphical validation confirmed WO's exceptional predictive accuracy. Figure 12a illustrates how closely WO's V-I and P-V curves align with simulated data, precisely capturing the electrical performance and maximum power point. Error analysis reinforced its high precision, with nearly all voltage prediction errors within a tight ± 0.05 V range. The rapid and consistent decrease in MSE towards the optimal solution, shown in Fig. 12b, demonstrates WO's efficient convergence. Finally, Fig. 12c, showcasing 100 independent runs, powerfully illustrates WO's remarkable robustness through its narrowest interquartile range, lowest median MSE, and absence of significant outliers, ensuring reliable and consistent performance.

Fuel cell sheet 10

To accurately model SOFC electrochemical behavior at 9 atm, the walrus optimization (WO) algorithm was deployed to determine seven critical parameters. This optimization aimed to reduce the Mean Squared Error (MSE) between model predictions and actual experimental voltage–current (V–I) data.

The results, summarized in Table 12, clearly establish WO's superiority over nine competing algorithms. WO achieved the best performance metrics, including the lowest minimum MSE (3.98E−05), highest stability (standard deviation, 0.934517), fastest execution time (0.320533 s), and the top Friedman ranking test score (1.5625).

Further graphical validation confirmed WO's exceptional predictive accuracy. Figure 13a illustrates how closely WO's V-I and P-V curves align with simulated data, precisely capturing the electrical performance and maximum power point. Error analysis reinforced its high precision, with nearly all voltage prediction errors within a tight ± 0.05 V range. The rapid and consistent decrease in MSE towards the optimal solution, shown in Fig. 13b, demonstrates WO's efficient convergence. Finally, Fig. 13c, showcasing 100 independent runs, powerfully illustrates WO's remarkable robustness through its narrowest interquartile range, lowest median MSE, and absence of significant outliers, ensuring reliable and consistent performance.

Conclusion

This study was able to establish the walrus optimization (WO) algorithm as a highly effective and robust tool for the precise identification of unknown parameters in solid oxide fuel cell (SOFC) models. The main goal was to minimize the mean squared error (MSE) between the model's output voltage predicted by the model and empirical experimental data. The proposed methodology was thoroughly validated in 10 different operational scenarios, which covered a broad range of temperatures (1073 to 1273 K) and pressures (1 to 9 atm). Comprehensive comparisons against nine established metaheuristic algorithms proved the superior performance of the WO algorithm, always attaining the lowest MSE values, fastest computational times, and highest statistical ranking, as confirmed by Friedman tests. The excellent agreement between the V-I and P-V curves of the WO-optimized model and experimental data, the small error distributions, and uniform convergence characteristics demonstrate the accuracy and reliability of the model in the electrochemical characteristics of SOFCs.

Despite its proven success, this work has some limitations that open the way for future research. A main limitation is the consideration of a particular electrochemical model under steady-state conditions. The performance of the WO algorithm in finding parameters for dynamic, transient, or degraded SOFC models is still an open question. Furthermore, although the algorithm demonstrated remarkable efficiency, its computational performance was assessed on a particular hardware configuration; its scalability to ultra-large-scale optimization problems or its implementation on embedded systems for real-time control needs to be explored.

Future work will be guided along a number of promising paths. Firstly, the application of the WO algorithm will be extended to parameter identification for dynamic models of SOFCs and other fuel cell technologies, Proton Exchange Membrane Fuel Cells (PEMFCs). Secondly, research will be conducted on the integration of the identified high-fidelity SOFC models into system-level simulations for grid integration studies and the development of advanced model predictive control strategies. Finally, attempts will be made to hybridize the WO algorithm with local search techniques in order to further improve its exploitation capabilities and to rigorously test its performance on a wider set of complex engineering optimization problems other than energy systems.

Author contributions MKS, MS: Conceptualization, Methodology, Software, Data curation, Formal analysis, Investigation, Resources, Visualization, Validation, and Writing-original draft preparation. PJ; RK: Conceptualization, Methodology, Software, Resources, Data curation, Funding, Validation, Visualization, and Writing-original draft preparation. A., RJ: Formal analysis, Investigation, Validation, Visualization, and Writing-review and editing. MKS: Formal analysis, Supervision, Visualization, and Writing-review and editing.

Data availability This manuscript does not report any data generation or analysis.

Declarations

Ethics approval Not applicable

Informed consent Not applicable

Conflict of interest The authors declare no competing interests.

References

1. Alam M, Kumar K, Verma S, Dutta V (2020) Renewable sources based DC microgrid using hydrogen energy storage: modelling and experimental analysis. Sustain Energy Technol Assess 42:100840
2. Verma S, Kumar K, Das LM, Kaushik SC (2021) Effect of hydrogen enrichment strategy on performance and emission features of biodiesel-biogas dual fuel engine using simulation and experimental analyses. J Energy Resour Technol 143(9):092301
3. Hosseini SH, Tsolakis A, Alagumalai A, Mahian O, Lam SS, Pan J, Peng W, Tabatabaei M, Aghbashlo M (2023) Use of hydrogen in dual-fuel diesel engines. Prog Energy Combust Sci 98:101100
4. Khajuria R, Yelisetti S, Lamba R, Kumar R (2024) Optimal model parameter estimation and performance analysis of PEM electrolyzer using modified honey badger algorithm. Int J Hydrogen Energy 49:238–259
5. Kumar K, Alam M, Dutta V (2021) Energy management strategy for integration of fuel cell-electrolyzer technologies in microgrid. Int J Hydrogen Energy 46(68):33738–33755
6. Ćalasan M, Aleem SHA, Hasanien HM, Alaas ZM, Ali ZM (2023) An innovative approach for mathematical modeling and parameter estimation of PEM fuel cells based on iterative Lambert W function. Energy 264:126165
7. Khajuria R, Lamba R, Kumar R (2022) Optimal parameter extraction and performance analysis of proton exchange membrane fuel cell. In 2022 IEEE international conference on power electronics, drives and energy systems (PEDES) (pp. 1–6). IEEE
8. Zhang B, Wang R, Jiang D, Wang Y, Wang J, Ruan B (2023) Parameter identification of proton exchange membrane fuel cell based on swarm intelligence algorithm. Energy 283:128935
9. Rizvandi OB, Braun R (2025) Distinct modeling parameter identification for precision modeling of solid oxide cells under fuel cell and electrolysis modes. J Power Sources 653:237716
10. Fathy A, Rezk H (2022) Political optimizer based approach for estimating SOFC optimal parameters for static and dynamic models. Energy 238:122031
11. Khajuria R, Lamba R, Kumar R, Yelisetti S (2022) Application of metaheuristic techniques in optimal parameter estimation of solid oxide fuel cell. In: International conference on advances in energy research. Springer Nature Singapore, Singapore, pp 605–613
12. Xing Y (2023) Adaptive parameter estimation. Modeling and control strategies for a fuel cell system. Springer International Publishing, Cham, pp 83–133
13. Khajuria R, Lamba R, Kumar R (2023) Model parameter extraction for PEM electrolyzer using honey badger algorithm. In: 2023 IEEE 3rd international conference on sustainable energy and future electric transportation (SEFET). IEEE, pp 1–6
14. Wang J, Xu YP, She C, Xu P, Bagal HA (2022) Optimal parameter identification of SOFC model using modified gray wolf optimization algorithm. Energy 240:122800
15. Guo H, Gu W, Khayatnezhad M, Ghadimi N (2022) Parameter extraction of the SOFC mathematical model based on fractional order version of dragonfly algorithm. Int J Hydrogen Energy 47(57):24059–24068
16. Hao P, Sobhani B (2021) Application of the improved chaotic grey wolf optimization algorithm as a novel and efficient method for parameter estimation of solid oxide fuel cells model. Int J Hydrogen Energy 46(73):36454–36465
17. Bai Q, Li H (2022) The application of hybrid cuckoo search-grey wolf optimization algorithm in optimal parameters identification of solid oxide fuel cell. Int J Hydrogen Energy 47(9):6200–6216
18. Kele C, Xinmei W, Youssefi N (2022) Model parameter estimation of SOFCs using a modified cat optimization algorithm. Sustain Energy Technol Assess 52:102176
19. Zhang M, Xu Z, Lu X, Liu Y, Xiao Q, Taheri B (2021) An optimal model identification for solid oxide fuel cell based on extreme learning machines optimized by improved red fox optimization algorithm. Int J Hydrogen Energy 46(55):28270–28281
20. Xiong G, Zhang J, Shi D, Zhu L, Yuan X (2021) Optimal identification of solid oxide fuel cell parameters using a competitive hybrid differential evolution and Jaya algorithm. Int J Hydrogen Energy 46(9):6720–6733
21. Yousri D, Hasanien HM, Fathy A (2021) Parameters identification of solid oxide fuel cell for static and dynamic simulation using comprehensive learning dynamic multi-swarm marine predators algorithm. Energy Convers Manag 228:113692
22. Ba S, Xia D, Gibbons EM (2020) Model identification and strategy application for solid oxide fuel cell using rotor hopfield neural network based on a novel optimization method. Int J Hydrogen Energy 45(51):27694–27704
23. Xiong G, Zhang J, Shi D, Yuan X (2020) A simplified competitive swarm optimizer for parameter identification of solid oxide fuel cells. Energy Convers Manag 203:112204
24. Yang B, Wang J, Zhang M, Shu H, Yu T, Zhang X, Yao W, Sun L (2020) A state-of-the-art survey of solid oxide fuel cell parameter identification: modelling, methodology, and perspectives. Energy Convers Manage 213:112856
25. Han W, Li D, Yu D, Ebrahimian H (2023) Optimal parameters of PEM fuel cells using chaotic binary shark smell optimizer. Energy Sources Part A Recovery Util Environ Eff 45(3):7770–7784
26. Wang N, Wang D, Xing Y, Shao L, Afzal S (2020) Application of co-evolution RNA genetic algorithm for obtaining optimal parameters of SOFC model. Renew Energy 150:221–233
27. El-Hay EA, El-Hameed MA, El-Fergany AA (2019) Optimized parameters of SOFC for steady state and transient simulations using interior search algorithm. Energy 166:451–461
28. Yang B, Guo Z, Yang Y, Chen Y, Zhang R, Su K, Shu H, Yu T, Zhang X (2021) Extreme learning machine based meta-heuristic algorithms for parameter extraction of solid oxide fuel cells. Appl Energy 303:117630
29. Shi H, Li J, Zafetti N (2020) RETRACTED: New optimized technique for unknown parameters selection of SOFC using converged grass fibrous root optimization algorithm, 1428–1437
30. Abaza A, El Sehiemy RA, Bayoumi ASA (2020) Optimal parameter estimation of solid oxide fuel cell model using coyote optimization algorithm. In: Recent advances in engineering mathematics and physics: proceedings of the international conference RAEMP 2019. Springer International Publishing, pp 135–149
31. Bagal HA, Soltanabad YN, Dadjuo M, Wakil K, Zare M, Mohammed AS (2021) SOFC model parameter identification by means of modified African vulture optimization algorithm. Energy Rep 7:7251–7260
32. Jia H, Taheri B (2021) Model identification of solid oxide fuel cell using hybrid Elman neural network/quantum pathfinder algorithm. Energy Rep 7:3328–3337
33. Hachana O, El-Fergany AA (2022) Efficient PEM fuel cells parameters identification using hybrid artificial bee colony differential evolution optimizer. Energy 250:123830
34. Khajuria R, Lamba R, Kumar R (2022) Parameters extraction of PEMFC model using evolutionary based optimization algorithms. In: International conference on advances in energy research. Springer Nature Singapore, Singapore, pp 443–451

35. Fathy A, Rezk H, Alharbi AG, Yousri D (2023) Proton exchange membrane fuel cell model parameters identification using chaotically based-bonobo optimizer. Energy 268:126705
36. Vaze R, Deshmukh N, Kumar R, Saxena A (2021) Development and application of quantum entanglement inspired particle swarm optimization. Knowl-Based Syst 219:106859
37. Deshmukh N, Vaze R, Kumar R, Saxena A (2023) Quantum entanglement inspired grey wolf optimization algorithm and its application. Evol Intell 16(4):1097–1114
38. Abdollahzadeh B, Khodadadi N, Barshandeh S, Trojovský P, Gharehchopogh FS, El-kenawy ESM, Mirjalili S (2024) Puma optimizer (PO): a novel metaheuristic optimization algorithm and its application in machine learning. Cluster Comput 27(4):5235–5283
39. Barua S, Merabet A (2024) Lévy arithmetic algorithm: an enhanced metaheuristic algorithm and its application to engineering optimization. Expert Syst Appl 241:122335
40. Tian Z, Gai M (2024) Football team training algorithm: a novel sport-inspired meta-heuristic optimization algorithm for global optimization. Expert Syst Appl 245:123088
41. Oladejo SO, Ekwe SO, Mirjalili S (2024) The hiking optimization algorithm: a novel human-based metaheuristic approach. Knowl-Based Syst 296:111880
42. Zhang J, Wu W, Mobayen S (2023) System identification of solid oxide fuel cell models using improved version of cat and mouse optimizer. Energy Sources Part A Recover Util Environ Eff 45(1):2553–2571
43. Ebrahimi SM, Hasanzadeh S, Khatibi S (2023) Parameter identification of fuel cell using repairable grey wolf optimization algorithm. Appl Soft Comput 147:110791
44. Ismael I, El-Fergany AA, Gouda EA, Kotb MF (2024) Cooperation search algorithm for optimal parameters identification of SOFCs feeding electric vehicle at steady and dynamic modes. Int J Hydrogen Energy 50:1395–1407
45. Chen K, Li J, Liu K, Bai C, Zhu J, Gao G, Wu G, Laghrouche S (2024) State of health estimation for lithium-ion battery based on particle swarm optimization algorithm and extreme learning machine. Green energy and intelligent transportation 3(1):100151
46. Li Y, Gao G, Chen K, He S, Liu K, Xin D, Luo Y, Long Z, Wu G (2025) State-of-health prediction of lithium-ion batteries using feature fusion and a hybrid neural network model. Energy 319:135163
47. Chen K, Luo Y, Long Z, Wang H, Li Y, Gao G, Wu G (2025) Battery state of health estimation using deep transfer learning on short-term charging data. Measurement. https://doi.org/10.1016/j.measurement.2025.118233
48. Zhang Y, Huang C, Huang H, Wu J (2023) Multiple learning neural network algorithm for parameter estimation of proton exchange membrane fuel cell models. Green Energy Intell Transp 2(1):100040
49. Han M, Du Z, Yuen KF, Zhu H, Li Y, Yuan Q (2024) Walrus optimizer: a novel nature-inspired metaheuristic algorithm. Expert Syst Appl 239:122413
50. Li Y, Wu Q, Zhu H (2015) Hierarchical load tracking control of a grid-connected solid oxide fuel cell for maximum electrical efficiency operation. Energies 8(3):1896–1916
51. Chuahy FD, Kokjohn SL (2019) Solid oxide fuel cell and advanced combustion engine combined cycle: a pathway to 70% electrical efficiency. Appl Energy 235:391–408
52. Lan T, Strunz K (2017) Multiphysics transients modeling of solid oxide fuel cells: methodology of circuit equivalents and use in EMTP-type power system simulation. IEEE Trans Energy Convers 32(4):1309–1321
53. El-Hay EA, El-Hameed MA, El-Fergany AA (2018) Steady-state and dynamic models of solid oxide fuel cells based on satin bowerbird optimizer. Int J Hydrogen Energy 43(31):14751–14761
54. Cao Y, Li Y, Zhang G, Jermsittiparsert K, Razmjooy N (2019) Experimental modeling of PEM fuel cells using a new improved seagull optimization algorithm. Energy Rep 5:1616–1625
55. Gotfredsen AB, Appelt M, Hastrup K (2018) Walrus history around the north water: human–animal relations in a long-term perspective. Ambio 47:193–212
56. Ray GC, Hufford GL, Overland JE, Krupnik I, McCormick-Ray J, Frey K, Labunski E (2016) Decadal Bering Sea seascape change: consequences for Pacific walruses and indigenous hunters. Ecol Appl 26(1):24–41
57. Jay CV, Olson TL, Garner GW, Ballachey BE (1998) Response of Pacific walruses to disturbances from capture and handling activities at a haul-out in Bristol Bay, Alaska. Mar Mamm Sci 14(4):819–828
58. Khishe M, Mosavi MR (2020) Chimp optimization algorithm. Expert Syst Appl 149:113338
59. Dehghani M, Mardaneh M, Malik OP (2020) FOA:'following'optimization algorithm for solving power engineering optimization problems. Journal of Operation and Automation in Power Engineering 8(1):57–64
60. Arora S, Singh S (2019) Butterfly optimization algorithm: a novel approach for global optimization. Soft Comput 23:715–734
61. Azizi M (2021) Atomic orbital search: a novel metaheuristic algorithm. Appl Math Model 93:657–683
62. Seyyedabbasi A, Kiani F (2023) Sand cat swarm optimization: a nature-inspired algorithm to solve global optimization problems. Eng Comput 39(4):2627–2651
63. Jia H, Li J, Song W, Peng X, Lang C, Li Y (2019) Spotted hyena optimization algorithm with simulated annealing for feature selection. IEEE Access 7:71943–71962
64. Dhiman G, Kumar V (2019) Seagull optimization algorithm: theory and its applications for large-scale industrial engineering problems. Knowl-Based Syst 165:169–196
65. Bairathi D, Gopalani D (2018) Salp swarm algorithm (SSA) for training feed-forward neural networks. In Soft Computing for Problem Solving: SocProS 2017, vol 1. Springer Singapore, pp 521–534
66. Mirjalili S, Lewis A (2016) The whale optimization algorithm. Adv Eng Softw 95:51–67